

# Applications of Artificial Intelligence/Machine Learning to High-Performance Composites

Yifeng Wang<sup>a,b</sup>, Kan Wang<sup>b</sup> and Chuck Zhang<sup>a,b\*</sup>

*<sup>a</sup>H. Milton Stewart School of Industrial and Systems Engineering, Georgia Institute of Technology, Atlanta, U.S.A.*

<sup>b</sup>*Georgia Tech Manufacturing Institute, Georgia Institute of Technology, Atlanta, U.S.A.*

\*Corresponding author: chuck.zhang@gatech.edu

## Abstract

With the booming prosperity of artificial intelligence (AI) technology, it triggers a paradigm shift in engineering fields including material science. The integration of AI and machine learning (ML) techniques in material science brings significant advancements in understanding and characterizing underlying physics. Due to the overall outstanding properties compared to conventional metallic materials, high-performance fiber reinforced polymer (FRP) composites have attracted great interest. This article aims to provide a comprehensive review of the state-of-the-art works of applying AI/ML methods in high-performance FRP composites, focusing on four critical stages throughout the product life cycle, i.e., design, manufacturing, testing, and monitoring. This present study covers the tasks of material development and selection, process modeling and optimization, material property prediction, and damage diagnosis and prognosis in the four stages, which are conducted with the aid of advanced AI/ML algorithms. An outlook for the incorporation of modern advanced AI/ML models into FRP composite research is provided by the identification of current challenges and potential future research directions.

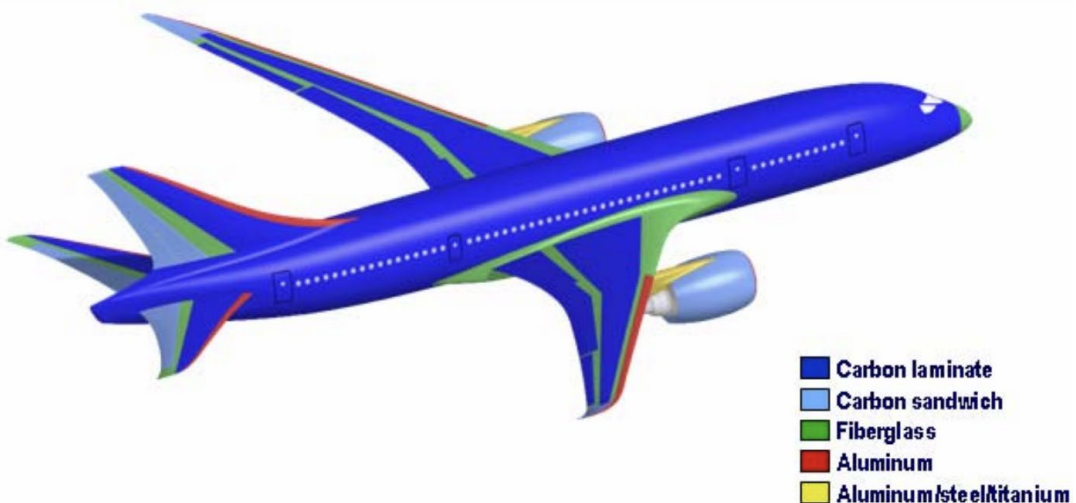
**Keywords:** Artificial intelligence; Machine learning; High-performance composites

## 1. Introduction

Recent advances in material science and engineering with the aid of modern computational algorithms and devices [1] have greatly pushed the need of advanced materials that can be adopted to increasingly complex engineering applications and adapted to multiple functional and safety requirements. Among various types of advanced materials such as crystal, metal alloy, etc., composite material, made up of at least two constituents into a heterogeneous mix [2], is one of the most promising structures. Upon an appropriate combination, the overall material performance will be enhanced, and characteristics of the

34 constituents will be kept simultaneously. Moreover, tailoring material properties can be  
35 achieved by adjusting the proportion, composition, structure and manufacturing accordingly  
36 [3-5]. Specifically, high-performance composites, which here refer to fiber reinforced  
37 polymers (FRPs) usually with carbon/glass fibers (CFRPs/GFRPs) and their joints, stand out  
38 due to their extraordinary properties such as higher strength, lighter weight, greater resistance  
39 to corrosion compared to conventional metallic materials, with a wide range of structural  
40 applications in aerospace [6-9], automobile [10, 11], marine [12, 13], renewable energy [14,  
41 15], and infrastructure industries [16]. For example, in the aircraft design, high-performance  
42 FRP composites provide an improvement in fuel-efficiency and emission reduction. In  
43 addition to functional benefits such as higher allowable hoop stress and corrosion resistances,  
44 a composite fuselage would allow more comfortable levels of cabin pressure and humidity  
45 which can effectively improve passenger comfort in modern commercial aircrafts such as  
46 Boeing 787 [17], as shown in Fig. 1. Besides, there are many aerospace components made of  
47 FRP composites even the primary structures are metallic [18].

48



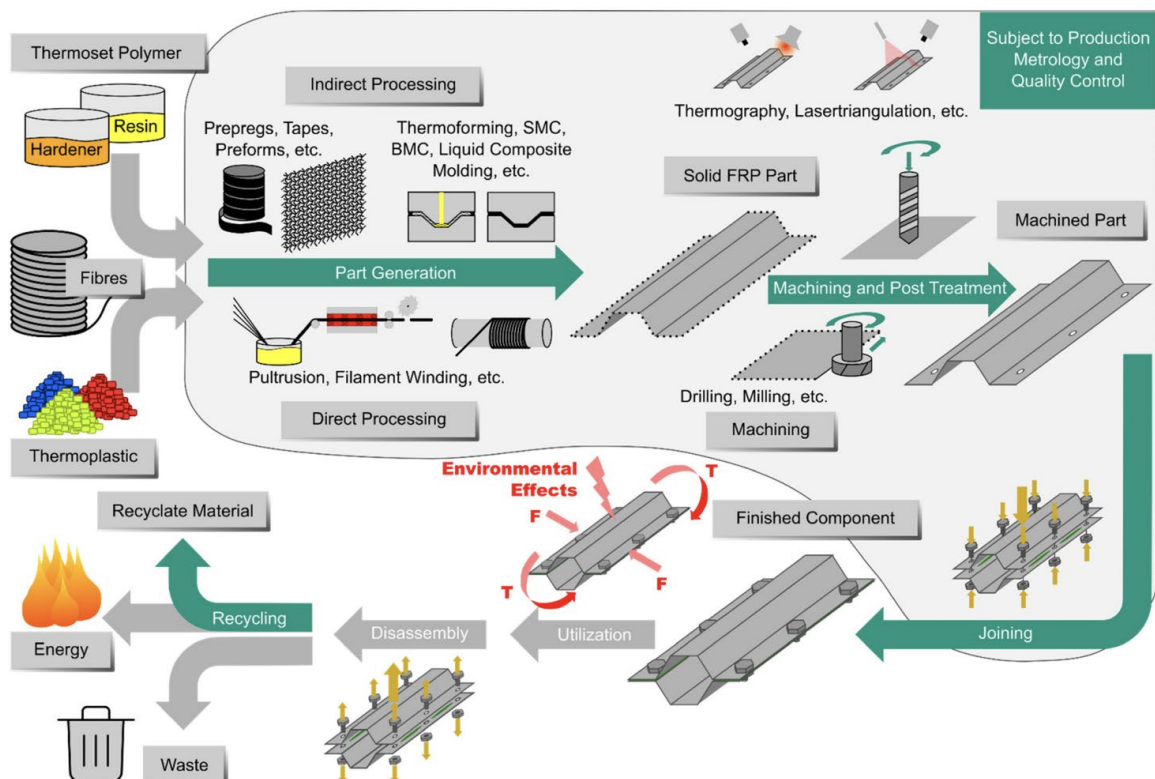
49

50 **Fig. 1.** Material usage in Boeing 787 where nearly 50% of components are composites [17].

51

52 The whole product life cycle of high-performance FRP composite structures is shown in  
 53 Fig. 2, including five main stages: designing, manufacturing (i.e., part generation, machining  
 54 and post treatment, and joining including curing), testing, monitoring, and recycling. Despite  
 55 of the outstanding advantages of material properties in various aspects, the complex multi-  
 56 stage manufacturing process (MMP) and the intricate material structure that leads to material  
 57 nonlinearity and anisotropy make it a challenging task to understand the material dynamics  
 58 and physics and characterize material behaviors [19]. Physics-based methods have long been  
 59 developed to analyze and understand the FRP composite materials in each stage of the MMP,  
 60 including both analytical models [20-23] and numerical simulations [24-31]. As analytical  
 61 models easily suffer from over-simplified assumptions, numerical simulations can achieve a  
 62 reasonable accuracy but often at the cost of computational resources.

63



64  
 65 **Fig. 2.** Product life cycle of FRP composite parts [32].  
 66

67        However, as there is abundant, even excessive, data produced and collected by the rapidly  
68        developing sensing technology in all life cycle activities, it has opened the door for artificial  
69        intelligence (AI), especially the machine learning (ML) technique due to the powerful data-  
70        processing capability. Numerous efforts have been made in applying AI/ML methods to the  
71        field of high-performance FRP composites, attempting to take the advantage of data-driven  
72        methods to address engineering problems. Existing studies on FRP composite structures with  
73        AI/ML techniques have mainly focused on surrogate modeling of finite element methods  
74        (FEMs) [33-35], physical process modeling [36-38], regression for property prediction [39-  
75        42], and signal/image-based classification [43-45]. Specifically, for instance, in the aerospace  
76        application of composite fuselage assembly, sparse learning models [46, 47] were proposed  
77        for the optimal placement of actuators and shape adjustment to reduce the maximum gap  
78        between two fuselages, significantly improving efficiency compared to traditional manual  
79        practice. Zhong et al. [48] further developed a finite element analysis (FEA) model-based  
80        automatic optimal shape control (AOSC) framework with model uncertainties addressed by  
81        cautious control.

82        Compared to traditional modeling methods of engineering problems such as analytical  
83        derivation and numerical simulations, AI/ML techniques generally require much less domain  
84        knowledge and are expected to discover underlying representative patterns in the dataset. For  
85        an intricate engineering problem that lacks adequate physical understanding like the adhesive  
86        joining of high-performance FRP composite structures, which is currently a common practice  
87        in aircraft manufacturing and repair but not fully proved due to its complexity, AI/ML can  
88        play a pivotal role in modeling, bypassing the requirement of thorough comprehension of its  
89        physical and chemical mechanism. State-of-the-art mechanical analysis of FRP composite  
90        adhesive joining is often under a simplified assumption that materials are linear elastic and  
91        isotropic [23]. Although one can set a more complex material setting in numerical analysis,

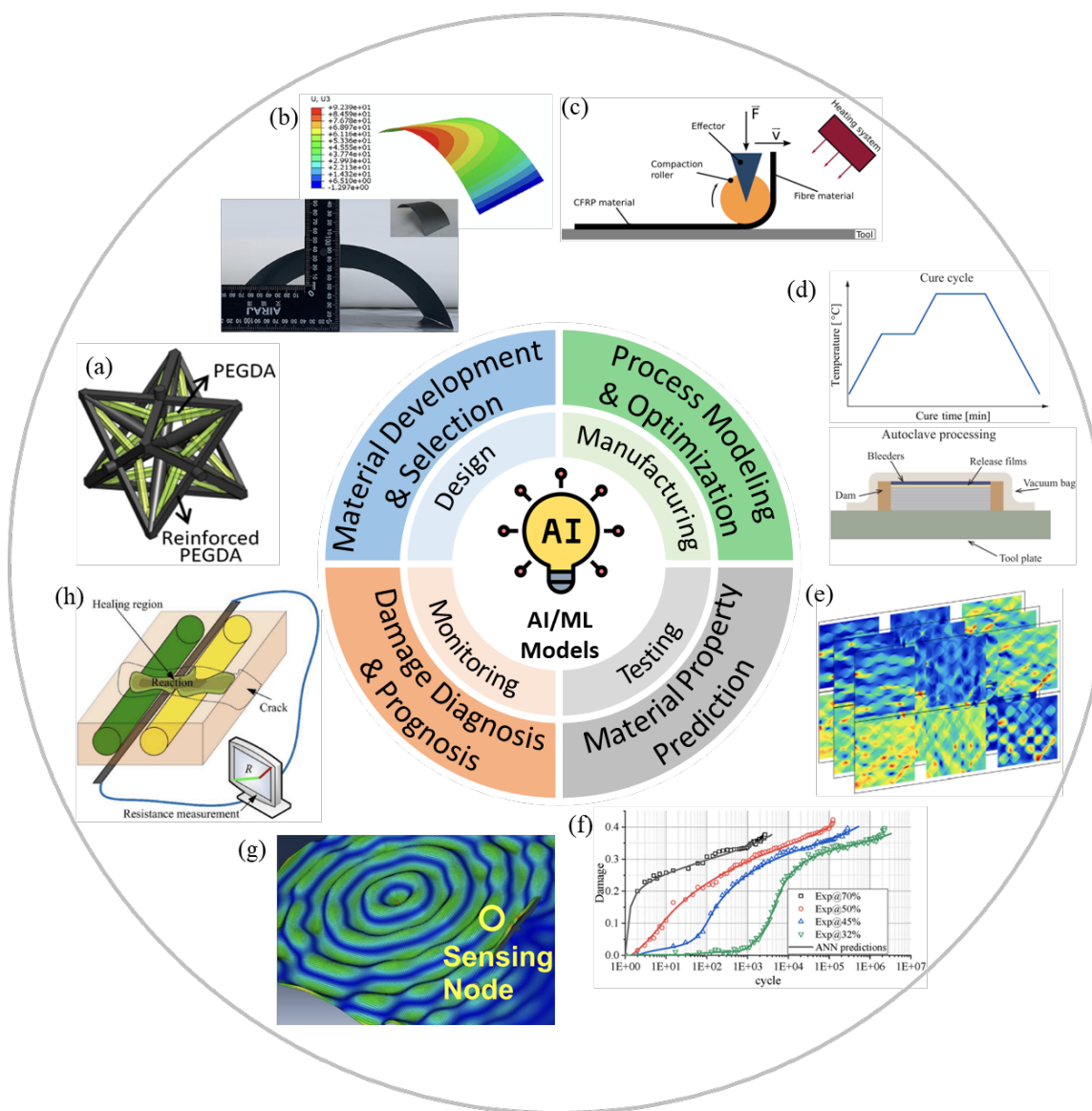
92 e.g., FEA, which is more consistent with reality [49, 50], an accurate result is usually at the  
93 cost of computational resources and time. On the other hand, once trained, AI/ML models  
94 take only a few seconds for prediction with a new input, which is much faster than traditional  
95 numerical simulations. Another prominent advantage of AI/ML methods over conventional  
96 ones is that data-driven algorithms have the potential to end-to-end model the whole MMP of  
97 high-performance FRP composites and adhesive joining given appropriate data pairs [39, 51].  
98 This is significantly important for quality-critical applications because the manufacturing  
99 parameters are control inputs and of great interest. Analytical and numerical models usually  
100 cannot capture this relation due to the unknown interactions between stages of MMP. In spite  
101 of these advantages, AI/ML models suffer from data-related issues which will be discussed in  
102 Section 7.2 in detail.

103 However, there is still a research gap in thoroughly understanding all the life cycle  
104 activities of FRP composite structures, especially the stages of designing, manufacturing,  
105 testing, and monitoring which substantially affect the in-service performance of FRP  
106 composites. A comprehensive article is highly desired that bridges the widespread and  
107 advanced AI/ML techniques for the engineering production and applications of high-  
108 performance FRP composites. Therefore, as shown in Fig. 3, this study summarizes current  
109 state-of-the-art adoption of AI/ML methods in design, manufacturing, testing, and monitoring  
110 stages of high-performance FRP composite structures with tasks of material development and  
111 selection, process modeling and optimization, material property prediction, and damage  
112 diagnosis and prognosis, respectively.

113 Hereafter, the rest of this article is organized as follows: section 2 provides a brief history  
114 of the development of AI/ML methods and their general applications in engineering. Section  
115 3 describes current utilization of AI/ML models in the material development and selection of  
116 composites with a focus on the framework of material genome initiative and inverse design.

117 The process modeling and optimization for the manufacturing processes including both part  
 118 generation and curing processes with the aid of AI/ML techniques are reviewed in section 4.  
 119 Section 5 considers the characterization of FRP composites, especially on the mechanical  
 120 properties of strength and fatigue, using AI/ML algorithms. Section 6 discusses the state-of-  
 121 the-art works for damage diagnosis and prognosis of composite structures that are integrated  
 122 with AI/ML methods. Section 7 concludes this review and looks forward to the prospects and  
 123 challenges by presenting potential future research directions.

124



125

126 **Fig. 3.** AI/ML models in design, manufacturing, testing, and monitoring stages of high-  
127 performance FRP composite structures with tasks of material development and selection,  
128 process modeling and optimization, material property prediction, and damage diagnosis and  
129 prognosis, respectively, where (a) Composite structure with tunable negative thermal  
130 expansion through computational design [52]; (b) FRP composite structure with simulation  
131 result to minimize PID through inverse design [53]; (c) AFP process for FRP composite part  
132 generation [54]; (d) Autoclave curing process with cure cycle of FRP composite structure  
133 [38]; (e) Microscopic stress tensor field maps of FRP composites for prediction [55]; (f)  
134 Stiffness degradation of composite laminates under cyclic loadings predicted by ANN [56];  
135 (g) Simulation of propagating Lamb wave with deformation magnification for NDI of FRP  
136 composites [57]; and (h) Integrated self-monitoring and self-healing design of CFRP  
137 structure for SHM [58].

138

## 139 **2. Development of AI/ML for Engineering**

140 Artificial intelligence (AI) is the field of computer science that studies how machines can  
141 be made to act intelligently [59], involving human-like psychological skills such as  
142 perception, association, prediction, planning, motor control, etc., with diverse information-  
143 processing capacities [60]. With a narrow definition, machine learning (ML), as a subfield of  
144 study in AI, investigates algorithms and statistical models that computer systems utilize to  
145 perform a specific task, e.g., classification, regression, clustering, etc., without being  
146 explicitly programmed [61].

147 The AI technology has long been developed since McCulloch and Pitts [62] proposed the  
148 MP neuron model, connecting nervous activity with computation in 1940s. Classic AI models  
149 were later extensively explored such as perceptron [63, 64], back-propagation technique [65],  
150 LeNet [66], LeNet-5 [67], support vector machine (SVM) [68, 69], k-nearest neighbor (kNN)

151 [70], long short-term memory (LSTM) [71], and etc., in which many of the landmark goals  
152 had been achieved.

153 AI, especially ML techniques, thrived when it entered the 21st century. Various concepts  
154 derived from ML, e.g., active learning [72], deep learning (DL) [73], physics-informed  
155 machine learning (PIML) [74], meta-learning [75], incremental learning [76], and etc., were  
156 proposed and developed to strengthen learning ability and deal with real engineering  
157 problems. In terms of implementation, one of the most powerful ML models is the neural  
158 network (NN). Numerous advanced artificial neural network (ANN) structures were explored  
159 including deep neural network (DNN), convolutional neural network (CNN) [66], AlexNet  
160 [77], ResNet [78], region-based CNN [79-82], recurrent neural network (RNN) [71, 83-85],  
161 generative adversarial network (GAN) [86-88], attention mechanism [89, 90], physics-  
162 informed neural network (PINN) [91], generative AI [92] for multiple tasks such as  
163 classification, pattern recognition, clustering, prediction and sequence processing.

164 In addition to the booming development of generic ML models, AI/ML models  
165 specifically designed for real engineering problems have also been extensively explored.  
166 Generally, the applications of AI/ML models to engineering can be divided into two parts: (1)  
167 AI/ML models help in computational modeling of complex physical systems, especially  
168 those with multi-physics interactions or unknown physics; and (2) Post-processing of  
169 experimental data can be conducted through advanced AI/ML models given their powerful  
170 data-mining capabilities.

171 In the domain of computational modelling, one of the most important goals is to build a  
172 simulator with a good balance between computational cost and simulation accuracy. Physics-  
173 based simulators by the first principle are usually able to achieve very high accuracy yet  
174 suffer from costing huge computational resources. While ML-based models can retain such  
175 computational advantage and dramatically reduce the required time when properly trained on

176 related physically-simulated data [93]. ANN has been successfully used to simulate the phase  
177 change of crystal materials based on molecular dynamics [94, 95] in the microscale, and  
178 turbulent flow dynamics [96, 97] macroscopically. Another significant application of AI/ML  
179 methods is surrogate modeling to perform downstream tasks such as real-time prediction,  
180 characterization, system health monitoring and control. AI/ML models have been extensively  
181 employed for estimating mechanical properties of composite materials and adhesives [39, 51,  
182 98], prediction of compressive strength of concrete [99], real-time anomaly detection on  
183 aircrafts [100], understanding transient physics of 2D fluid system [101, 102], and many  
184 other aspects. Recent advances in PIML have fostered massive applications to various  
185 engineering systems by incorporating known or partially known physics, which can be  
186 expressed in a set of ordinary/partial differential equations (ODEs/PDEs) into a machine  
187 learning framework. Hot topics are about fluid and thermal dynamics where PIML has great  
188 potential to emulate system dynamics for different applications, such as curing of composite  
189 systems [37, 38, 103] and weather system [104].

190 Post-processing of experimental data is also critical in engineering problems. AI/ML  
191 algorithms have long been utilized in biology and related fields to analyze large-scale data  
192 about molecules, proteins and genes by clustering [105-107] and using CNNs [108, 109]. In  
193 other fields such as composites [110-113], astronomy [114], cybersecurity [115], researchers  
194 are proactively exploring new applications of AI/ML methods as well.

195

### 196 **3. AI/ML in Material Development and Selection of High-Performance 197 Composites**

198 The incorporation of AI/ML into material science has brought new vigor and vitality,  
199 enabling more innovation in material development and selection, including the field of high-  
200 performance composites. One breakthrough is that deep generative models such as diffusion

201 models are applied to create novel crystal material representations at micro level by exploring  
202 latent feature spaces with the aid of fundamental physical law, e.g., quantum mechanics [116,  
203 117]. Although such models have not been extensively employed in the field of composites,  
204 it is expected that deep generative models would advance the discovery of better FRP  
205 composite materials with appropriate adaptation. The recent applications of AI/ML methods  
206 in material genome initiative and inverse design for composites will be discussed in this  
207 section.

### 208 ***3.1 AI/ML in Material Genome Initiative for High-Performance Composites***

209 Material Genome Initiative (MGI) is a federal multi-agency program that has been  
210 advanced to push the development of computational material science since its announcement  
211 in 2011 [118]. MGI is designed to accelerate the pace of discovery, design, deployment, and  
212 engineering of advanced materials via high-throughput experimentation (HTE) which is a  
213 technique that highly integrated with theory, experiment, and computation [119], where  
214 AI/ML models can be potentially applied for higher computational efficiency and accuracy.  
215 Along with the prosperity of AI/ML over the past decade, MGI has already enabled  
216 significant advances in material science with numerous applications. Utilizing high-  
217 throughput virtual screening (HTVS) that combines quantum chemical calculations, machine  
218 learning techniques, and cheminformatics methods, Gómez-Bombarelli et al. [120] explored  
219 over one million candidates in molecular space to identify promising novel design of organic  
220 light-emitting diodes (OLEDs). The selected candidates were experimentally demonstrated to  
221 reach state-of-the-art external quantum efficiencies.

222 In addition to advanced materials in the molecular level, MGI has profoundly impacted  
223 the progress in many other fields of materials, e.g., composites. Wang et al. [52] designed  
224 three-dimensional composite structures with tuneable negative thermal expansion through  
225 multi-material projection micro-stereolithography in the framework of computational design

226 that is advanced by MGI. Liu et al. [121] reported an HTE method that was used on  
227 functional composite hydrogels to facilitate rapid high-throughput screening of composition-  
228 property relationships, enabling accelerated engineering with optimized properties for  
229 processability and performance, which was proved by application to different functional  
230 composite hydrogel systems.

231 Although MGI has numerous successes in expediting discovery and development of new  
232 advanced functional materials including some composites, there is still a gap in the area of  
233 high-performance composites. The HTE method combined with powerful computation ability  
234 provided by ML algorithms has a great potential to optimize the design of high-performance  
235 FRP composite materials by searching for better combinations of reinforcement and matrix  
236 materials in terms of both composition and structure.

### 237 ***3.2 AI/ML in Inverse Materials Design of High-Performance Composites***

238 Unlike structure- and element-oriented design that are usually under some constraints,  
239 inverse design begins from a required functionality and searches for an ideal material  
240 structure [122]. Kim et al. [123] proposed a DNN-RNN-based encoder-decoder structure for  
241 the inverse design of organic molecules. The generated molecular structures achieved good  
242 agreement with the targeted triplet excitation energy of OLEDs in a later experimental  
243 validation.

244 Not only in design of molecular structures, but researchers also applied inverse design to  
245 composite materials, especially high-performance ones. Nomura et al. [124] used topology  
246 optimization specifically with tensor field variables on the fiber orientation to obtain beam  
247 structures with minimum compliance. Topology optimization was also employed by Jung et  
248 al. [125] to search for optimal spatially-varying fiber size and orientation in a multiscale  
249 manner in order to minimize structure compliance. AI/ML algorithms were successfully  
250 utilized in the inverse design process of high-performance composites, covering more

251 complex physical functionalities. Luo et al. [53] integrated FEM and ANN to perform  
252 prediction and inverse design of thermosetting-matrix composites of an asymmetric laminate  
253 for a targeted maximum process-induced distortion (PID). The resultant composite of carbon  
254 fiber and epoxy agreed with the targeted maximum PID with a root mean square error  
255 (RMSE) of 8.01%. Considering random uncertainty, Song et al. [126] firstly developed  
256 Kriging surrogate models to learn the transfer functions of both laminated and 2D-woven  
257 composites and employed a genetic algorithm (GA) to solve the inverse optimization design  
258 to achieve desired mechanical properties with minimum statistical deviation. Liu et al. [40]  
259 applied optimization algorithms for inverse design based on a deep operator network  
260 (DeepONet) that is designated to bridge the gap between mechanical behaviors and design  
261 space of hierarchical composites.

262 Extensive research works have shown the benefit of incorporating AI/ML algorithms into  
263 conventional inverse design and engineering of composite materials. However, this  
264 innovative approach demands a great generalization ability of AI/ML methods that can find  
265 novel material structures not included in existing databases. Current works in the field of  
266 high-performance composites mainly focus on utilizing AI/ML for surrogate modeling to  
267 represent the mapping from design space to the desired functionality, and then employing a  
268 separate optimization method for inverse design. A holistic approach that integrates these two  
269 steps is anticipated to achieve better performance. To this end, generative AI models have  
270 great potential to overcome the inherent limitations of finiteness of material choices in  
271 material databases. Specifically, combining variational autoencoders (VAEs) with diffusion  
272 models can be one of the prospective ML structures, which is able to generate novel material  
273 representations in the latent space, as demonstrated in [116]. Translating this strategy into  
274 composites domain and incorporating composite-specific physics knowledge is expected to  
275 contribute remarkable advances.

276

277 **4. AI/ML in Manufacturing Process Modeling and Optimization of High-  
278 Performance Composites**

279 Manufacturing of high-performance FRP composites parts and components involves part  
280 generation process and joining process by various techniques and methods. One of the  
281 pioneering works on composite manufacturing process modeling is the utilization of PIML  
282 and PINN which integrate physics and engineering knowledge into the framework of data-  
283 driven ML modeling, e.g., for composite curing process [37, 38, 103, 127]. This section will  
284 introduce both conventional and advanced manufacturing processes of FRP composites and  
285 review the state-of-the-art applications of AI/ML methods in it.

286 **4.1 AI/ML in Part Generation Process Modeling and Optimization of High-  
287 Performance Composites**

288 The part generation process of FRP composites is the process to reinforce matrix material  
289 with fiber preforms that are usually made by weaving, knitting, braiding, and stitching of  
290 fibers in sheet structure [128]. Conventional generation processes generally include injection  
291 molding, compression molding, liquid composite molding (resin transfer molding, rotational  
292 molding, and wet pressing), fiber deposition (automated tape/fiber placement), pultrusion,  
293 thermoforming, and filament winding. With the integration of AI/ML techniques into the  
294 manufacturing processes, higher production efficiency with less defects can be achieved by  
295 process modeling, monitoring, and optimization thanks to the powerful data processing  
296 capability of AI/ML algorithms.

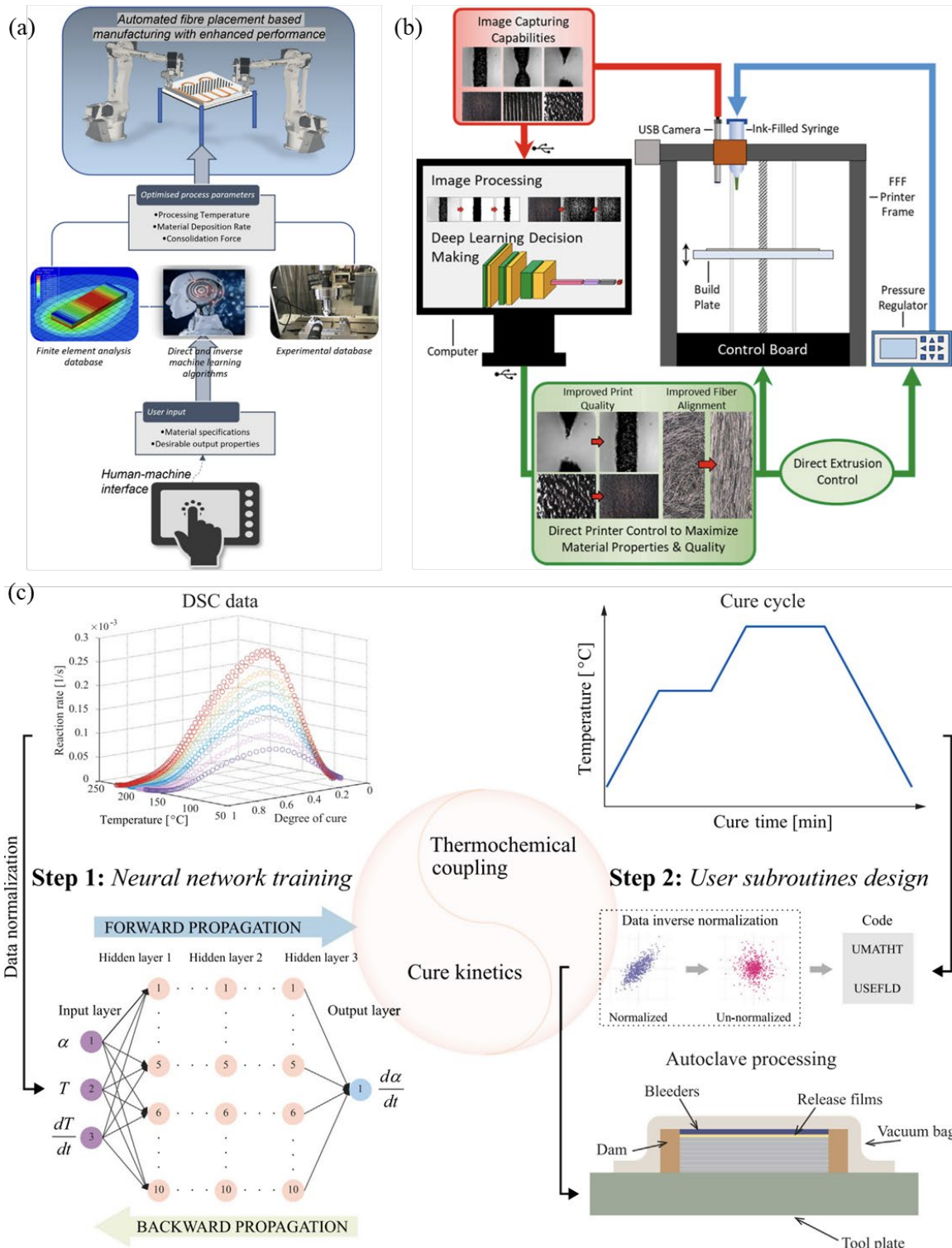
297 Image processing techniques have been actively applied into the automated fiber  
298 placement (AFP) process for layup defect detection and segmentation [54]. Zambal et al.  
299 [129] trained a CNN by images artificially generated by a probabilistic graphical model to  
300 mitigate the issue of data scarcity of some new defect types, where the trained model

301 achieved a 95% accuracy on real laser sensor data in AFP process for defect segmentation  
302 and classification. Thermal images were employed by Schmidt et al. [45] to comprehensively  
303 evaluate CNNs with three various architectures. Sacco et al. [130] presented their Advanced  
304 Composite Structures Inspection System (ACSiS) based on ANN for automated AFP defect  
305 detection, classification, and documentation. Meister et al. [131] investigated the relevance of  
306 certain image pixels regarding the decision-making response of a CNN classifier through  
307 explainable AI methods smooth integrated gradients and deep learning important features  
308 with Shapley additive explanations (DeepSHAP) to guide monitoring strategies in AFP  
309 inspection. In order to find optimized AFP process parameters given desirable mechanical  
310 properties, Islam et al. [132] proposed a hybrid approach which combines benefits of ANN,  
311 virtual sample generation (VSG) method, and physics-based numerical simulation with real  
312 data, as shown in Fig. 4(a).

313 On the other hand, additive manufacturing (AM) is one of the leading and advanced  
314 technologies in composite manufacturing for its flexibility in selection of fiber volume and  
315 orientation and ability to adapt to complex geometry. Broadly speaking, FRP composites that  
316 are additively manufactured can be categorized into continuous-fiber reinforced composites  
317 (by fused filament fabrication, laminated objective manufacturing), short-fiber reinforced  
318 composites (by material extrusion processes, vat photopolymerization processes, powder bed  
319 fusion processes, binder jetting), and voxelated polymeric composites (uniquely by AM  
320 approaches such as multiple jet fusion, and direct ink writing) [133]. AI/ML techniques have  
321 significantly improved AM processes, especially in process modeling and optimization.  
322 Yanamandra et al. [134] utilized a refined RNN with LSTM architecture to identify the fiber  
323 orientation in each layer to capture the tool-path information so as to reverse engineer a FRP  
324 composite made by fused filament fabrication (FFF). With the aid of Gaussian process  
325 regression (GPR), Hu et al. [135] thoroughly analyzed mechanical properties of polylactic

326 acid (PLA) composites with reinforcement of chopped long carbon fiber (CF) via fused  
327 deposition modeling (FDM) fabrication. Wright et al. [136] developed a novel closed-loop  
328 DL-integrated extrusion AM system to perform in-situ imaging and process parameter  
329 optimization on milled CF-reinforced polymeric composite by several CNNs to maximize  
330 material properties and quality, as shown in Fig. 4(b). The composite parts manufactured by  
331 direct ink writing (DIW) using the autonomously determined optimal parameters were  
332 inspected to be defect-free, demonstrating the effectiveness of the DL-DIW process  
333 optimization framework. A similar closed-loop robot-based AM system for real-time defect  
334 detection and parameter adjustment of CFRPs enabled by advanced CNN models, e.g.,  
335 YOLOv4, was proposed by Lu et al. [137].

336



337

338 **Fig. 4.** (a) Process flow diagram indicating the steps from user-input to ML process  
 339 optimization to AFP-based manufacturing [132]; (b) Overview of the DL-DIW framework  
 340 showing how a computer, FFF printer, and USB camera are interconnected to perform in-situ  
 341 parameter optimization [136]; (c) Flow chart of the cure process analysis via ANN including

342 cure kinetics and thermochemical coupling using non-isothermal differential scanning  
343 calorimetry (DSC) data [38].

344

345 **4.2 AI/ML in Curing Process Modeling and Optimization of High-**

346 **Performance Composites**

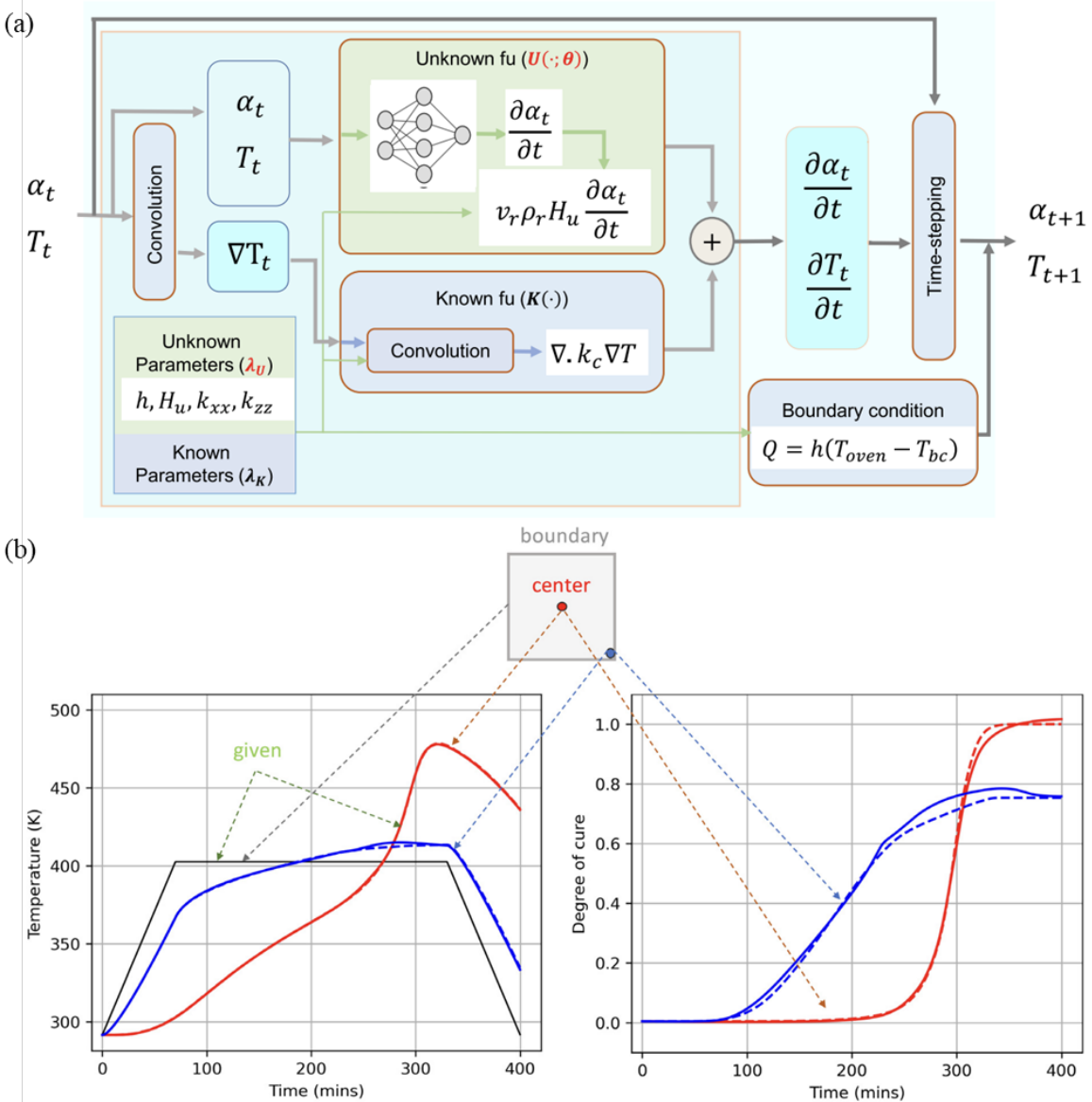
347 Once the FRP parts are manufactured, joining them together is the next step to make a  
348 component. In addition to traditional joining methods, e.g., mechanical fasteners such as  
349 riveted or bolted joints, and welding, adhesive joining is getting increasingly prevalent for  
350 composite parts due to its weight reduction and avoiding material damage and stress  
351 concentrations. The necessary step to join composite parts with adhesive films or pastes is to  
352 cure them. Not only happening during part generation, but the curing process also occurs in  
353 the joining processes of polymeric composites. However, residual stress will be generated  
354 during this process due to intrinsic factors of material and extrinsic cure conditions, possibly  
355 leading to defects like crack, delamination, distortion, and degradation of mechanical  
356 performance [138]. Understanding the physics of curing process and evolution of curing-  
357 induced residual stress is thus critical to improve the quality of FRP composites. Yet the  
358 curing process and corresponding residual stress and process-induced deformation (PID) are  
359 often complex interactions between thermal-chemical, flow-compaction, and thermal-  
360 mechanical properties of the fiber and matrix materials [139], AI/ML methods play a pivotal  
361 role in such research problems, fostering the understanding of complicated physics through a  
362 data-driven point of view.

363 ANNs have already been used in early attempts to model the curing kinetics and predict  
364 related parameters such as retained mass [140], degree of cure (DoC) [36], and time  
365 derivative of DoC [141]. Kim and Zobeiry [142] developed an ANN to identify equivalent 1-  
366 D cases for the 2-D geometry to speed up process simulation considering both geometric and

367 cure cycle parameters. Zobeiry and Poursartip [143] investigated three different scenarios of  
368 curing, i.e., to predict thermal lag or exotherm in a curing composite part on an either inert or  
369 metallic tool using theory-guided ML which takes physics-based features and uses a physics-  
370 based rationale to choose activation functions. Hui et al. [38] considered both cure kinetics  
371 and thermochemical coupling in building an ANN to predict the evolution of the DoC. As  
372 shown in Fig. 4(c), the predicted curing dynamics can be further used to guide the FE  
373 analysis or experiments.

374 With the advent of PIML and PINN, physical dynamics that are described by  
375 ODEs/PDEs can be emulated with higher efficiency and accuracy by incorporating the  
376 physics law into the loss function or ML model structure. Zobeiry and Humfeld [127] utilized  
377 a PINN to solve the conductive heat transfer PDE along with convective heat transfer PDEs  
378 as boundary conditions (BCs) of a heating composite part. Niaki et al. [37] modelled the  
379 thermochemical curing process considering exothermic heat transfer by creating two coupled  
380 PINNs for a bi-material composite-tool system. One PINN is to predict the DoC that is  
381 applicable to the composite material, while the other one is for the temperature distribution  
382 for both the tool and the composite part. Losses specially designed for boundary conditions  
383 were added to improve the performance of the PINN model. Akhare et al. [103] proposed a  
384 physics-informed neural differentiable (PiNDiff) model based on the pioneering PINN model  
385 Neural ODE to learn unknown physics from the limited indirect data and to infer unobserved  
386 variables and parameters in the application of composite curing. Based on a computational  
387 model of cure behaviour of a carbon/epoxy prepreg system proposed by Anandan et al. [22],  
388 the PiNDiff model for composite curing was structured as shown in Fig. 5(a) with a great  
389 performance on predicting curing dynamics of corner location of a square laminate when  
390 trained on temperature data collected at the center, as shown in Fig. 5(b).

391



392

393 **Fig. 5.** (a) Schematics of the PiNDiff module for the curing process; (b) PiNDiff predictions  
 394 on the temperature data collected at the center of the laminate, where black solid line  
 395 represents autoclave temperature that is the BC, red/blue solid line represents the prediction  
 396 at the center/corner location, red/blue dashed line represents the ground truth at the  
 397 center/corner location. (Reproduced from reference [103].)

398

399 A natural extension to process modeling is process optimization and control. Jahromi et al.  
 400 [144] formulated a nonlinear programming (NLP) problem to develop multi-linear-stage cure  
 401 cycles by minimizing the maximum temperature difference through the cure cycle to improve

402 the mechanical properties and gain a curing uniformity, by using a RNN for surrogate  
403 modeling. Struzziero and Teuwen [145] tackled the multi-objective optimization of the cure  
404 stage of the vacuum assisted resin transfer molding (VARTM) process for wind turbine  
405 blades, aiming to minimizing process time, spring-in, and maximum temperature overshoot  
406 by comparing the Pareto front obtained from GA. A ML framework, CompML (Composites  
407 Machine Learning), was used by Humfeld and Zobeiry [146] for active control of the  
408 composites autoclave processing. Specifically, two LSTM models were trained to solve the  
409 forward thermochemical problem to predict temperature histories of the part and tool, then  
410 the results were fed into a third ANN to search for an optimal cure cycle. Yuan et al. [33]  
411 built a surrogate model through radial basis function (RBF) of multi-field coupled FEM  
412 results and utilized a non-dominated sorting genetic algorithm-II (NSGA-II) to search for the  
413 global optimum solution where the cure time and maximum gradient of temperature and DoC  
414 are minimized to reduce the residual stress and improve production efficiency. Tang et al.  
415 [147] employed a multi-objective particle swarm optimization (MOPSO) algorithm to find an  
416 optimal cure cycle that minimizes total curing time, maximum difference of DoC, and spring-  
417 back angle of a C-shaped composite specimen after curing based on FEM simulations. The  
418 optimal cycle was later verified by an experiment to effectively shorten the curing time and  
419 reduce the spring-back angle.

420 Although various advancements have been made by AI/ML methods in the  
421 manufacturing and curing processes modeling and optimization of FRP composites, there are  
422 still areas not fully touched. One notable domain is to end-to-end model the whole  
423 manufacturing process including both part generation and curing processes to better link all  
424 related manufacturing parameters with the ultimate performance measures. PIML/PINN are  
425 specifically designed to be applied on physics-related problems, having a great potential for  
426 understanding the complex interactions during the manufacturing of composite materials.

427 **5. AI/ML in Material Property Prediction of High-Performance**

428 **Composites**

429 Typically, material properties encompass chemical (chemical composition, atomic  
430 bonding, corrosion resistance, etc.), electrical (conductivity, resistivity, dielectricity, etc.),  
431 magnetic (ferro/para/diamagnetism, etc.), thermal (thermal conductivity, expansion,  
432 diffusivity, etc.), mechanical (strength, stiffness, elasticity, plasticity, toughness, fatigue,  
433 ductility, brittleness, etc.), and optical (refraction, refraction, diffraction, etc.) aspects [148].  
434 Mechanical properties, among all these aspects, often hold significant importance since they  
435 characterize the material in most engineering applications. Traditional methods to determine  
436 the mechanical properties of a material rely on repeating mechanical tests laboriously, which  
437 is time-consuming and expensive. However, the utilization of AI/ML methods to predict  
438 material properties has experienced significant growth and released a large number of efforts  
439 from laborious tests for various materials including composites. The capacity to learn  
440 intricate nonlinearities has enabled AI/ML methods to encourage researchers to use them to  
441 perform these tasks. The main breakthrough in predicting mechanical properties of high-  
442 performance composite structures is to forecast the stress/strain tensor field maps instead of  
443 merely a value of strength, which requires a more sophisticated design of model to deal with  
444 the high-dimensional and multiscale data. CNN-based neural operator with multiscale FEM  
445 would be a good candidate [41, 55, 149-151]. This section will focus on the recent advances  
446 of AI/ML techniques for prediction of mechanical properties of high-performance composites,  
447 especially on strength and fatigue behavior of composites and their joints.

448 **5.1 AI/ML in Strength Prediction of High-Performance Composites**

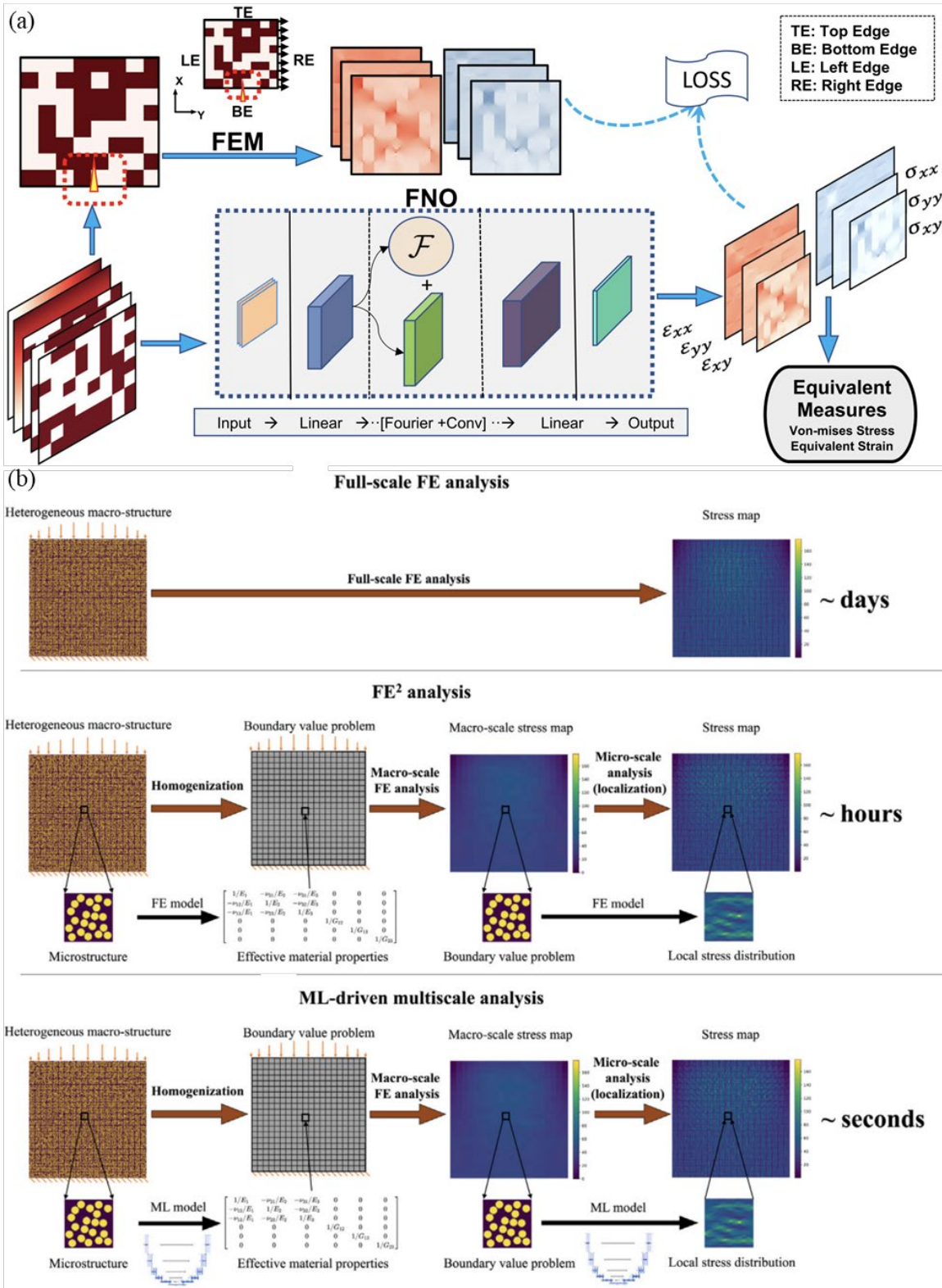
449 Strength of material is often recognized as the most important mechanical  
450 characterization for structural parts/components and engineering materials to which FRP  
451 composites are usually applied. Rahman et al. [152] built a CNN-based surrogate ML model

452 for molecular dynamics simulations to predict the shear strength of carbon nanotube-polymer  
453 interfaces. In addition to the interfacial properties in carbon nanotube (CNT) composites, the  
454 geometric deformation was investigated through a model that integrated functional PCA  
455 (FPCA) with DNN to ensure predictive performance and interpretability [153]. On the other  
456 hand, for general FRP composites, Abuodeh et al. [154] utilized a resilient back-propagating  
457 neural network (RBPNN) as a regressor to predict the shear strength of reinforced concrete  
458 (RC) beams strengthened with externally bonded FRP sheets. The recursive feature  
459 elimination (RFE) algorithm and neural interpretation diagram (NID) were later employed to  
460 identify significant parameters to improve predictive efficiency and accuracy. Yin and Liew  
461 [155] investigated the application of gradient boosting regressor (GBR) and ANN on  
462 evaluating the interfacial properties of FRP composites such as the interfacial shear strength  
463 (IFSS) and the maximum force given fiber geometries and basic mechanical properties of  
464 fiber and matrix materials. Li et al. [156] predicted the transverse microstructure-property  
465 relationship of unidirectional (UD) FRP composites with microvoids through an ML-  
466 combined material informatics approach where the principal component analysis (PCA) was  
467 used to extract statistical representations and a genetic algorithm optimized back propagation  
468 (GABP) neural network was built for prediction. A similar framework but with principal  
469 component regression (PCR) was employed by Olfatbakhsh and Milani [157] on fabric  
470 composites. Prediction and analysis of dynamic strength [158] and failure criteria [111] in  
471 terms of both maximum compressive and tensile stress using AI/ML methods were also  
472 explored.

473 Apart from predicting a single or several strengths that are in the form of scalar, FRP  
474 composite stress field prediction has caught great attention and been proactively explored  
475 recently [41, 55, 149-151]. Specifically, Rashid et al. [149] utilized the Fourier neural  
476 operator (FNO) to predict component-wise stress and strain for two-phase composites. As

477 shown in Fig. 6(a), the FNO learned the constitutive relation between the design geometry  
478 and different mechanical responses, predicting the normal and shear components of the stress  
479 and strain tensor field in an end-to-end fashion with the material microstructure alone as the  
480 input. Notably, the FNO framework was demonstrated to have a decent generalization ability  
481 to unseen microstructure geometries. Gupta et al. [55] reported an ML-based approach for  
482 multiscale mechanics modeling considering microstructural heterogeneity where a CNN with  
483 U-Net architecture was trained to learn the mapping between the spatial arrangement of fibers  
484 and corresponding 2D stress tensor fields. Three different approaches for predicting the stress  
485 field of a heterogeneous macro-structured composite and a comparison of computational time  
486 are shown in Fig. 6(b). The U-Net model trained for stress prediction in the microstructure  
487 was tested successfully on three different macro-structures of varying sizes and subjected to  
488 different loading and boundary conditions, showing the capability for multiscale analysis.

489



490

491 **Fig. 6.** (a) The workflow of FNO framework for predicting stress and strain field, where the  
 492 2D digital composite geometry is analyzed for the mode-I tensile test using FEM with a pre-  
 493 crack along the  $x$ -direction and loading in the  $y$ -direction, and the tensor components are

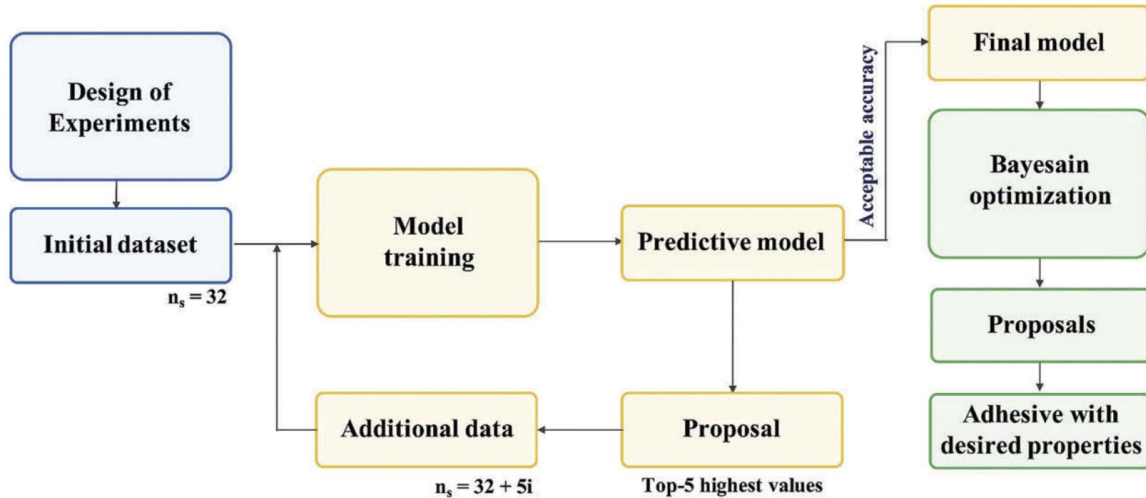
494 used to derive scalar-valued equivalent measures such as von-mises stress and equivalent  
495 strains [149]; (b) Multiscale mechanics modeling of a heterogeneous macro-structure using  
496 three different approaches: (i) full-scale FE analysis, (ii)  $FE^2$  analysis, and (iii) ML-driven  
497 multiscale analysis. The full-scale FE analysis is the least efficient, the multiscale FE analysis  
498 is parallelizable and more efficient, and the ML-driven multiscale analysis is the most  
499 efficient [55].

500

501 In addition to predicting strength of FRP composite itself, research on forecasting  
502 strength and failure analysis on composite adhesive joints has also been extensively explored  
503 for its critical significance in multiple engineering applications. Not only the structural epoxy  
504 adhesives [39, 159], but also the whole bonded joints, e.g., interfacial properties, are of great  
505 research interest, with various types of mechanical testing for different fractures such as  
506 mode-I [51], mode-II [160-164], and mixed-mode [113, 165, 166], and the adhesion between  
507 different materials [167, 168]. ANN is the most used model among all the AI/ML algorithms,  
508 combined with FEM utilizing cohesive zone model (CZM) that describes composite adhesion  
509 by a traction-separation law given some certain simplified assumptions, to predict shear and  
510 peel strength of composite adhesive joints and perform failure analysis. This combined model  
511 directly links nominal material properties (usually from datasheet) and joint geometries to the  
512 mechanical characterization, effectively improving the prediction efficiency compared to  
513 FEM alone. The potential of applying advanced AI/ML models has been explored as well.  
514 Considering the issue of small dataset that is common in engineering applications, Pruksawan  
515 et al. [159] utilized an active learning framework with gradient boosting as the regressor and  
516 Bayesian optimization for final proposing for a combination of epoxy parameters that yield a  
517 maximum adhesive joint strength. This active learning framework will augment the training  
518 dataset by adding additional data proposed by the predictive model from the original design

519 space, as shown in Fig. 7, which runs in an iterative supervised manner and would generate a  
 520 highly uniform set of sample points. This property of active learning is expected to mitigate  
 521 the issue of lack of training data in a real engineering problem such as FRP composites.

522



523

524 **Fig. 7.** Flowchart of the active learning approach for modeling and optimization of epoxy  
 525 adhesive [159].

526

## 527 **5.2 AI/ML in Fatigue Prediction of High-Performance Composites**

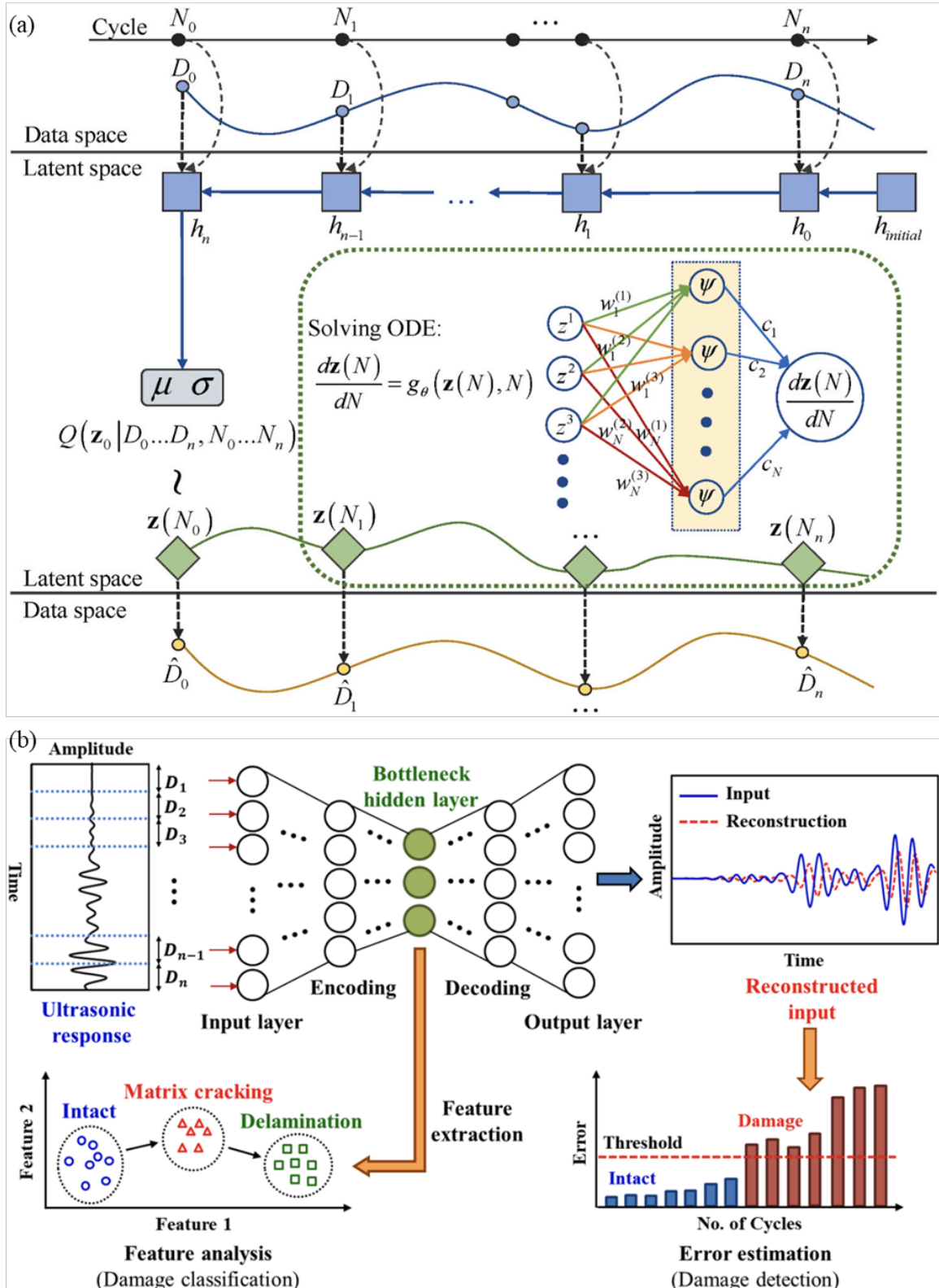
528 Compared to the strength of material, fatigue characterizes the behavior and failure of a  
 529 material due to a cyclic loading other than a quasi-static one, which is also the most common  
 530 material failure modes that harm the safety of structural components [169]. Fatigue data is  
 531 often noisy and unapproachable for physics-based methods to get an accurate result, which is  
 532 suitable for AI/ML analysis. Fatigue life prediction is a widely studied topic in the literature  
 533 where researches apply AI/ML models to the fatigue analysis of composites, attempting to  
 534 bridge material and experimental parameters and the fatigue life [42, 170-174]. Other aspects  
 535 have also been extensively analyzed, with more concentrations on the fatigue behavior  
 536 characterization, e.g., damage/crack evolution [112, 175], strength/stiffness degradation [56,  
 537 176], and fatigue diagnosis and prognosis [34, 177-179].

538 Based on the strain pattern obtained from distributed optical fiber sensors bonded on a  
539 CFRP double cantilever beam (DCB) specimen under a cyclic loading, Cristiani et al. [175]  
540 built a one-dimensional (1D) and a two-dimensional (2D) CNN which were separately  
541 trained to predict the delamination length due to fatigue loading to track the crack evolution.  
542 Notably, as shown in Fig. 8(a), Tao et al. [56] applied a  $\beta$ -variational autoencoder ( $\beta$ -VAE)  
543 firstly to extract and disentangle the latent features to represent the underlying driving  
544 mechanism of stiffness degradation, and then adopted the Neural ODE framework to learn  
545 the dynamics of the latent features. The Neural ODE framework predicts the stiffness of the  
546 composite laminate over the cycle-domain continuously, achieving a better accuracy than a  
547 conventional phenomenological model. Lee et al. [179] built a deep autoencoder (DAE)-  
548 based model, as shown in Fig. 8(b), to detect and classify fatigue damage in composite  
549 structures using the ultrasonic signals collected from the CFRP plate under ultrasonic Lamb  
550 waves. The DAE was trained to reconstruct the ultrasonic signals obtained when the sample  
551 was intact and for testing, the reconstruction RMSE was selected as an index to detect  
552 damage once it exceeded the determined threshold. On the other hand, the feature learned by  
553 the hidden layer of the DAE was extracted for damage classification by a density-based  
554 spatial clustering of applications with noise (DBSCAN) algorithm after processed by singular  
555 value decomposition (SVD) for dimension reduction.

556 Composite materials exhibit complex hierarchical structures, and thus their mechanical  
557 properties depend on interactions at multiple length scales. It is expected to predict material  
558 properties with improved accuracy and better understanding of the connection between the  
559 structure and properties if an AI/ML model is adopted which considers multi-scales, e.g.,  
560 from nanoscale to micro- and macroscale, and with considerable interpretability. Additionally,  
561 neural operator (NO), other than ordinary neural network, has a great potential on predicting  
562 more complex material properties based on material structure and some basic properties, e.g.,

563 as demonstrated in [149], because it is able to map between input and output functions on  
564 continuous domains and do super-resolution on the output instead of just mapping between  
565 input and output points on a fixed, discrete grid [180]. This special nature enables NO  
566 overcome the inherent issue of lacking enough continuous data in engineering applications.

567



568

569 **Fig. 8.** (a) Computation graph of the ANN model based on the Neural ODE structure with  $\beta$ -  
 570 variational autoencoder ( $\beta$ -VAE) [56]; (b) Overview of the deep autoencoder-based fatigue  
 571 damage detection and classification for composite structures [179].

572 **6. AI/ML in Damage Diagnosis and Prognosis of High-Performance**  
573 **Composites**

574 With the increasing use of high-performance composite parts and components in real life,  
575 it is of great importance to maintain the structural integrity by damage detection and  
576 evaluation not only during manufacturing processes, but also when they are in service.  
577 Comprehensive diagnostic and prognostic for FRP composites are critically significant for  
578 safety concerns, yet particularly challenging due to non-homogeneity and anisotropy of  
579 composite materials [181]. Generally, diagnosis is to obtain a clear picture of the health state  
580 of the material, and prognosis will estimate the remaining useful life (RUL) [35]. Therefore,  
581 robust and reliable non-destructive inspection (NDI) methods are essential and highly  
582 desirable for detection of various types of damages. On the other hand, structural health  
583 monitoring (SHM) performs an in-situ and continuous damage evaluation of composite  
584 structures, and thus has the potential to identify defects in the early stages, allowing for a  
585 timelier maintenance and repair [182]. Although performing a reliable NDI and SHM on FRP  
586 composite is difficult because of intricate structural nature, AI/ML methods shed a light by  
587 the powerful data analysis capabilities. For example, weak adhesion and kissing bonds are the  
588 defects in composite laminates and adhesive joints that are extremely difficult to detect non-  
589 destructively through conventional techniques and yet very safety-concerning. AI/ML models,  
590 on the other hand, with appropriate feature extraction based on physical knowledge, perform  
591 decently on a binary classification task to determine the existence of such defects [110].  
592 Recent advancements in utilizing state-of-the-art AI/ML methods for NDI and SHM on high-  
593 performance composites will be reviewed in this section.

594 **6.1 AI/ML in Non-Destructive Inspection of High-Performance Composites**

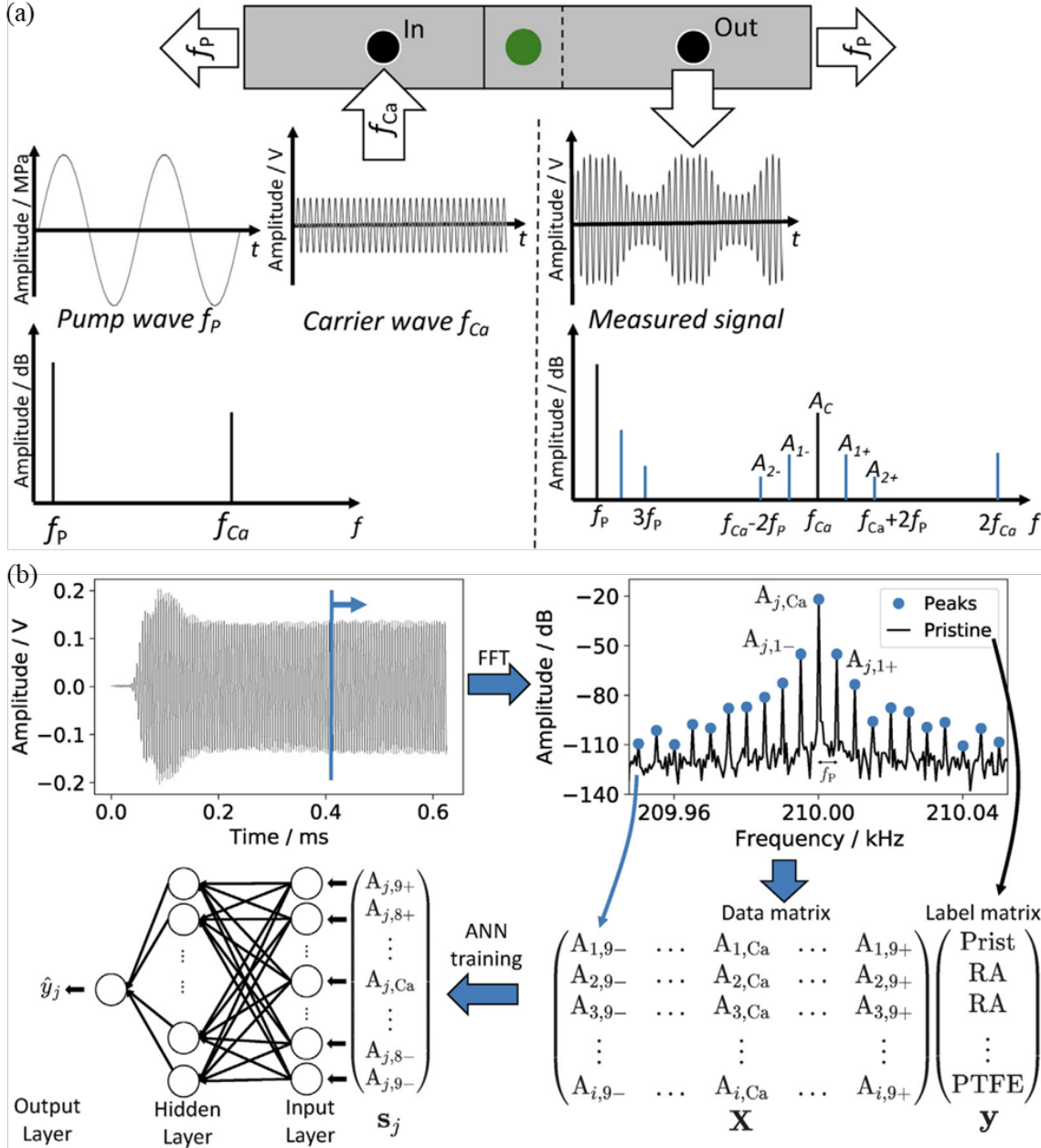
595 Generally, based on the output signal for analysis and its frequency, NDI techniques can  
596 be categorized into three main groups: acoustic wave-based, electromagnetic techniques-

597 based, and imaging techniques-based [183]. AI/ML methods, especially ANNs and CNNs,  
598 have been applied to these specific fields for composite defect and damage inspection,  
599 detection, localization, and classification. Acoustic wave-based NDI mainly includes acoustic  
600 emission (AE) [184] and ultrasonic testing (UT) using Lamb waves [185, 186], guided waves  
601 [187, 188], and etc., which are suitable for monitoring and locating cracking and  
602 delamination in FRP composites. Defects such as crushing and impact that are explicitly on  
603 the surface are easily detected by visual inspection (VI), which has also been aided by  
604 ANNs/CNNs for automation and better visual detectability for defects that are negligible for  
605 naked eyes [189, 190]. Apart from VI and eddy current testing (ECT) [191], another  
606 important NDI method in the electromagnetic techniques-based group is infrared  
607 thermography (IRT). Combined with different AI/ML methods, e.g., hierarchical clustering  
608 [192], kNN [193], Faster R-CNN with attention mechanism [194], IRT is able to detect the  
609 size and location of defects in composite laminates based on thermal images in an automated  
610 manner. The third group imaging techniques-based NDI generally utilizes the difference  
611 between images obtained at different time to highlight changes in defects, including  
612 shearography and digital image correlation (DIC) for measuring strain and displacement  
613 [195, 196], and X-ray computed tomography (CT) with the capacity to obtain information  
614 about internal porosity, pores shape, dimension, and etc. [197]. Additionally, Gillespie et al.  
615 [198] utilized the transient thermal conduction profiles to detect delamination in composite  
616 laminates based on a supervised support vector classification (SVC) algorithm.

617 Although AI/ML algorithms have been extensively applied to detect defects and flaws in  
618 composite structures, the area of composite adhesive joints, e.g., damages and weak adhesion,  
619 has not been fully explored due to its intricate and invisible nature. Kissing bond, defined as a  
620 “zero-volume disbond” [199] that the adhesive and adherend are in contact without voids and  
621 chemical and/or molecular bonds between the surfaces, is one of the most interested and

622 safety-concerning defects of composite adhesive joints. Because the defect locates in the  
623 bondline, i.e., in the interface between two non-transparent materials, and the considerable  
624 thickness of adherends compared to that of adhesive, ordinary visual methods and those  
625 depending on subtle deformation of a thin part are challenging to be applied. Despite of such  
626 difficulties, multiple physics-based methods, especially based on ultrasonic signals, were  
627 developed [200-202]. AI/ML methods are also under proactive exploration. Boll et al. [110]  
628 employed an ANN to classify kissing bonds made by release agent from pristine samples and  
629 defective specimen with a polytetrafluoroethylene (PTFE) film inserted and predict the shear  
630 strength of these three types of bonding based on vibroacoustic modulation (VAM) analysis.  
631 Specifically, as shown in Fig. 9(a), an ultrasonic Lamb-wave signal  $f_{Ca}$  with a high-strain  
632 pump wave  $f_p$  will result in a signal modulation and sidebands through the bonding area. The  
633 material nonlinearity introduced by defects and induced under a high-strain load is expected  
634 to further modulate the ultrasonic Lamb wave, revealing higher harmonics than pristine  
635 samples. As illustrated in Fig. 9(b), the sidebands and carrier amplitudes after a fast Fourier  
636 transform (FFT) were selected as the input of the ANN model for defect classification and  
637 shear strength prediction. With the aid of ML classifiers such as SVM, ultrasonic signals that  
638 obtained from different NDI methods such as pulse-echo immersion [43], phased array [203]  
639 and ordinary UT [204] were utilized to extract physics-based features for classification of  
640 adhesive bonding.

641



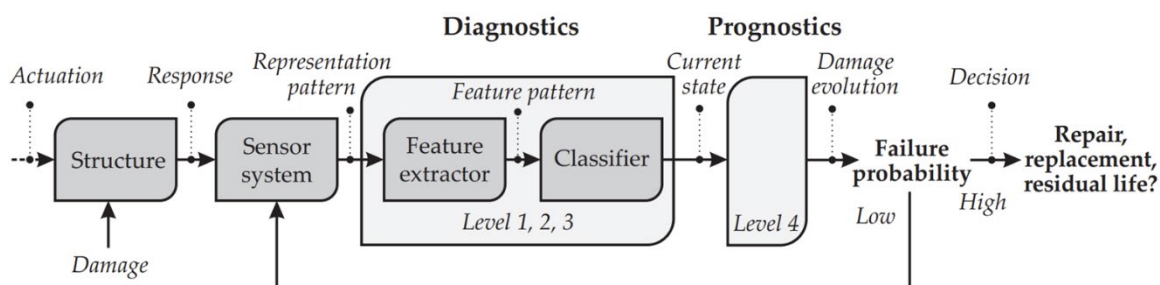
643 **Fig. 9.** (a) Schematic representation of a VAM analysis, where combining a high-strain pump  
 644 wave  $f_p$  with an ultrasonic Lamb-wave as signal carrier  $f_{Ca}$  results in a signal modulation and  
 645 sidebands, and the piezoceramic of the carrier signal (In) is excited at  $f_{Ca}$  and resulting  
 646 vibrations are received by another piezoceramic actuator (Out); (b) Exemplary illustration of  
 647 the ANN approach used to analyse VAM signals, where the Prist, RA and PTFE are  
 648 corresponding labels of pristine specimen and specimen with release agent contamination or  
 649 a PTFE-film, respectively. (Reproduced from reference [110].)

650

651 **6.2 AI/ML in Structural Health Monitoring of High-Performance Composites**

652 Taking NDI technique as core a component, SHM provides a continuous and in-situ  
653 monitoring of structural loads and damages and environmental parameters, sensing structural  
654 state parameters such as stress and/or strain [205]. Selecting a proper sensor and designing an  
655 appropriate way to embed the sensor into composite structures without harming structural  
656 integrity and strength too much are the primary task and challenge of SHM. The general  
657 workflow of SHM is depicted in Fig. 10. The SHM process consists of a diagnostic and a  
658 prognostic part where the former one estimates the current state of the structure or the system  
659 while the latter one evaluates the damage evolution and forecasts the remaining service life  
660 [35]. After diagnosis and prognosis of a system with adequate sensing ability, one can obtain  
661 the failure probability for downstream decision making about repair or replacement. There  
662 are also four performance levels of SHM defined by Rytter [206], namely, (1) verification of  
663 damage presence; (2) determination of damage location; (3) estimation of damage severity;  
664 and (4) prediction of remaining service life.

665



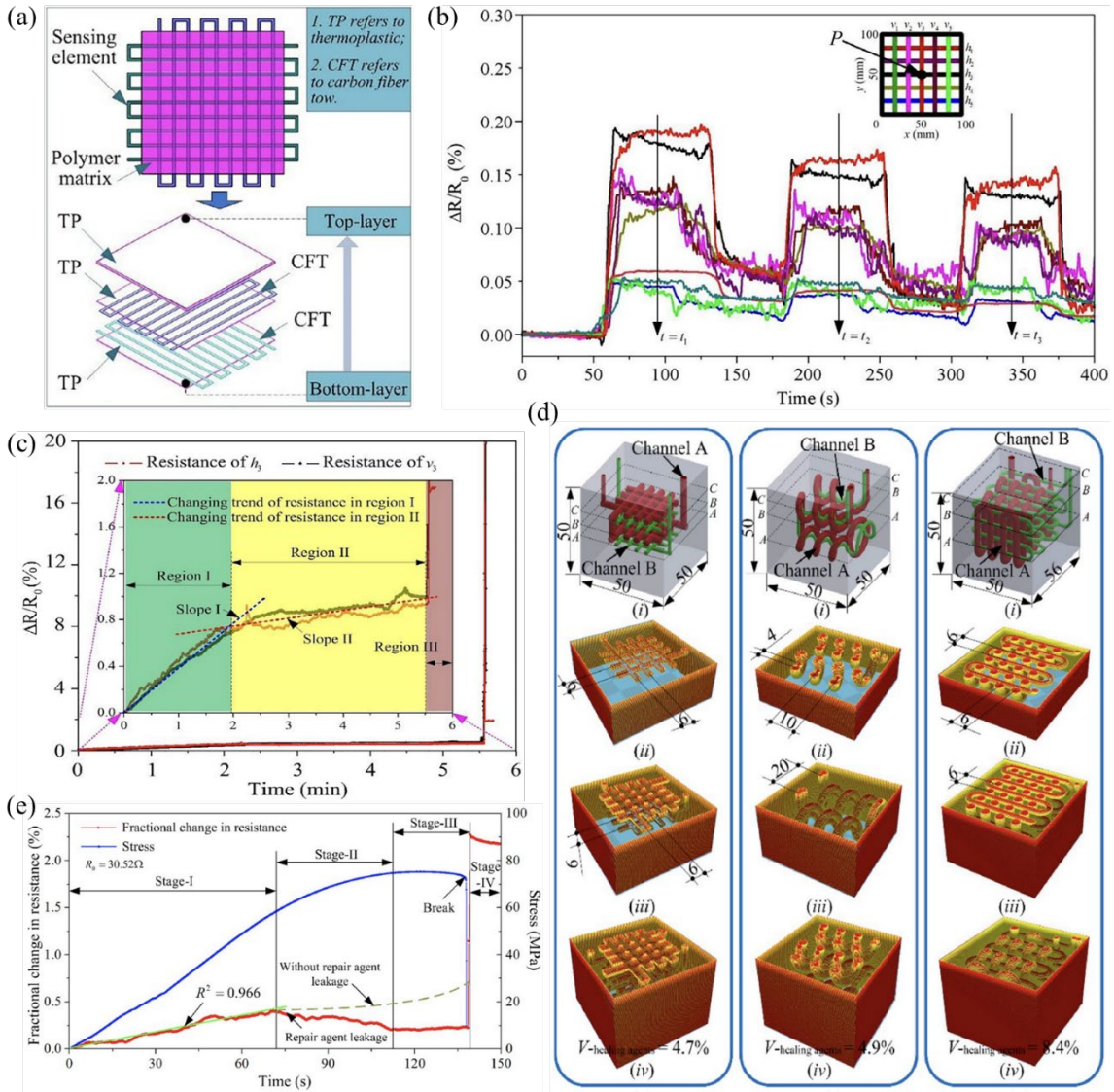
667 **Fig. 10.** The multidisciplinary structural health monitoring process [207].

668

669 With the development of advanced sensor technology, numerous physics-based SHM  
670 research have been done with various design and application of sensing strategies, e.g.,  
671 electromechanical impedance/resistance-based sensors [208-210], electric time domain

672 reflectometry [211, 212], fiber Bragg grating sensors [213], self-monitoring and self-healing  
673 [58], and etc. As shown in Fig. 11(a-c), a smart sensing grid that is comprised of continuous  
674 carbon fiber tows were integrated within the polymer matrix to identify the deformation field  
675 distribution and detect both micro- and macro-damage according to the dramatic change in  
676 the slope of fractional change in electrical resistance with the strain based on the electrical-  
677 mechanical behavior [210]. Luan et al. [58] pioneeringly designed a self-monitoring and self-  
678 healing composite structure with curing agent embedded using the dual-material AM  
679 technology, which is shown in Fig. 11(d), where the continuous carbon fibers serve as both a  
680 sensory element and reinforcement. Fig. 11(e) plots the result of three-point bending testing  
681 with four obvious stages. Damages can be detected depending on the change of the slope.

682



683

684 **Fig. 11.** (a-c) Schematic of a meshed smart structure and fabrication sequence (from bottom-  
685 layer to top-layer) with the testing result of fractional change in electrical resistance of each  
686 continuous carbon fiber tow, and a detailed look at the relation of middle tows that can be  
687 three apparent stages: elastic stage, micro-damage stage, and macro-damage stage [210]; (d,  
688 e) Specimens with plane-, spiral-, and interlock-type of self-healing structures, with a testing  
689 result of variation of fractional change in resistance and stress versus time for the continuous  
690 carbon fiber tow embedded specimen during the entire loading process [58].

691

692 AI/ML methods, e.g., ANN, SVM, kNN, etc., have been utilized to analyze the  
693 experiment data for downstream tasks such as damage detection, classification, and  
694 characterization for different composite structures [44, 57, 214-216]. Ewald et al. [57]  
695 proposed a CNN framework called DeepSHM which involves data augmentation of  
696 ultrasonic guided wave signals through wavelet transform and formalizes a generic method  
697 for end-to-end deep learning for defect classification. Liu et al. [214] performed a clustering  
698 analysis using the bisecting K-means algorithm to identify different damage modes for  
699 acoustic emission signal sources from a composite wind turbine blade. Khan et al. [215]  
700 investigated the classification of two types of delaminated samples from healthy ones using  
701 SVM with input of multi-level features extracted from various DL models through transfer  
702 learning. The raw structural vibration data was encoded into high-resolution time-frequency  
703 images using synchroextracting transforms (SETs). Reis et al. [216] employed an ANN  
704 model with input of mini-batches from the high-dimensional vibration data by dislocated  
705 series method to detect and classify delamination damage of composite beams. Diaz-Escobar  
706 et al. [44] evaluated the performance of different ML models including ANN, kNN, random  
707 forest (RF), and SVM on damage identification and characterization in composite laminates  
708 using the electrical resistance tomography (ERT) data.

709 NDI and SHM signals are usually high-dimensional data, leaving a great space for AI/ML  
710 algorithms due to their powerful data analysis and processing capabilities. Despite of recent  
711 advances in applying AI/ML methods to perform damage and defect detection, localization,  
712 and classification, and prediction of RUL for high-performance composite structures, current  
713 focuses are mainly on these downstream tasks. Integrating the manufacturing information  
714 such as parameters in part generation and curing processes is expected to improve the model  
715 performance as these information reveals inherent material properties. NDI and SHM may

716 also benefit from multi-model systems which incorporate multiple sensors and inspection  
717 methods.

718

## 719 **7. Conclusions and Future Scope**

### 720 **7.1 Conclusions**

721 AI/ML technologies have witnessed their rapid development where novel techniques  
722 sprout at an unprecedented rate, which triggers a paradigm shift in engineering including  
723 material science. How advanced materials are conceptualized, designed, manufactured, and  
724 tested is redefined enabled by the great computational power of high-dimensional data  
725 analysis and processing. High-performance FRP composite materials, with the advancements  
726 in material science and engineering, have been extensively applied to replace conventional  
727 structural materials in various industries such as aerospace, marine, automotive, and  
728 infrastructure. The intricate structure and complicated interaction inherent in FRP composite  
729 structures raise an obstacle to researchers for understanding material behaviors. The  
730 utilization and integration of AI/ML algorithms into the science and engineering of high-  
731 performance composites marks a pivotal advancement, providing a new understanding from  
732 the view of data analytics.

733 In the current era of innovation with the emergence of AI/ML techniques, this article  
734 provides a comprehensive review of recent advances and applications of AI/ML methods in  
735 the product cycle life activities of high-performance FRP composites including material  
736 development and selection, manufacturing, testing, defect and damage inspection, and in-  
737 service monitoring, as summarized in Table 1. The development of AI/ML techniques for  
738 science and engineering is briefly reviewed. The AI/ML-based MGI and inverse design of  
739 advanced materials are considered when discussing the application of AI/ML methods in  
740 material development and selection. Later, this review categorizes the manufacturing of FRP

741 composite structures into part generation and curing processes with an overview of process  
 742 modeling and optimization using AI/ML techniques. Predicting material properties utilizing  
 743 AI/ML models is then discussed with the emphasis on two significant mechanical properties,  
 744 i.e., strength and fatigue. In addition, this study goes over advances of the application of  
 745 AI/ML methods to the NDI and SHM of composite structures.

746

747 **Table 1.** Details of AI/ML models for design, manufacturing, testing and monitoring stages  
 748 of high-performance composites in the literature listed in this review.

Stage/Task	Application	Method
Design: Material Development and Selection	Customized material fabrication	MGI [52]
	Composite functionality optimization	High-Throughput Experimentation, Synthesis, Characterization [121]
	Inverse design for required functionality	DeepONet [40], ANN [53], Topology Optimization [124, 125], Kriging with GA [40, 126]
Manufacturing: Process Modeling and Optimization	AFP process optimization	CNN [45, 129, 131], ANN [130, 132]
	AM process modeling and optimization	GPR [135], Refined RNN with LSTM [134], CNN [136, 137]
	Curing process modeling	ANN [36, 38, 140-143], PINN [37, 127], Neural ODE [103]
	Curing process optimization and control	RBF Network with NSGA-II [33], RNN with NLP [144], Multi-Objective GA [145], ANN and LSTM [146], MOPSO Algorithm [147]
Testing: Material Property Prediction	Composite strength prediction	Sparse Regression [111], ANN [154, 155, 158], GABP Network with PCA [156], PCR [157]
	Composite stress field prediction	U-Net-based CNN [41, 55, 150, 151], FNO [149]
	Composite adhesive joint strength prediction	ANN [39, 51, 160, 163-165, 167, 168], GPR [113, 166], Active Learning [159], DNN and Genetic Programming [161], PINN [162, 163]
	Fatigue prediction and characterization	ANN [42, 171, 174], Neural ODE [56, 112], RNN [170], RF [172], Gradient Boosting [173], CNN [175], GA [176]
	Fatigue diagnosis and prognosis	ANN and Particle Filtering [34], SVM and RF [177], DNN [178], DAE [179]
Monitoring: Damage Diagnosis and Prognosis	Composite damage classification and detection	CNN [184, 186, 188, 189, 195-197], SVM and RF [185], ANN [187, 190, 191], Hierarchical Clustering [192], kNN [193], Faster R-CNN [194], SVC [198]
	Composite adhesive joint defect detection	SVM [43, 203, 204], ANN [110]
	Structural health monitoring	ANN [44, 216], CNN [57], K-Means [214], SVM [215]

749

750 **7.2 Issues of AI/ML and Potential Solutions**

751 There are certain drawbacks inherent in data-driven AI/ML models and limitations in the  
752 implementation and practice of adopting such algorithms in a complex engineering problem  
753 of high-performance composites. These shortcomings are summarized to point out the room  
754 for future improvements.

755 **7.2.1 Data Issues and Potential Solutions**

756 Lack of data, especially structured data, often impacts the successful utilization of AI/ML  
757 models which are usually data-hungry. Structured data in an appropriate form of input data  
758 and output label is highly desired for the application of the standard supervised learning.  
759 Because of the expensive cost of physically destructive testing and experiments of high-  
760 performance FRP composites, data scarcity and imbalance are one of the most common  
761 issues that hinder extensive deployment of AI/ML methods.

762 Data scarcity occurs generally in each activity during the life cycle of composite  
763 structures due to the expensive and time-consuming testing, and data imbalance can be often  
764 observed when considering defects and damages in process modeling, material properties  
765 prediction, and classification/localization tasks in NDI and SHM. In addition to the ordinary  
766 methods that deal with data imbalance such as stratified sampling, a reliable and robust data  
767 augmentation strategy is expected to address both issues of scarce and imbalanced data. Such  
768 a strategy can be a combination of conventional preprocessing of data, e.g., noise injection,  
769 transformation, filtering, etc. and generating synthetic data using advanced AI/ML models  
770 such as GAN and its variants.

771 Another issue related to data is the lack of paired labels. In the framework of supervised  
772 learning, it is often assumed that the input data and labels are balanced and paired, which is  
773 not reflective of the real-world scenarios where data acquisition and labelling processes are

774 not ideal. Labels can be noisy, incorrect, and/or incomplete, resulting in an inexact,  
775 inaccurate, and/or incomplete supervision. To address this issue, weakly-supervised learning  
776 is desirable that is designated to train ML models with limited, noisy, and/or imprecise  
777 labelling through data-driven methods [217]. Weakly-supervised learning has been applied to  
778 a variety of fields [218-221], but its potential in the area of high-performance composite  
779 structures has not been fully explored yet.

780 Considering complex engineering problems of FRP composites, data issues of scarcity,  
781 imbalance, labeling pose challenges to the effective and efficient application of AI/ML  
782 methods. Low data quality such as inaccurate manufacturing process parameters, testing  
783 measurements with large uncertainties requires researchers to cautiously acquire and/or  
784 collect data needed. Limited data will degrade AI/ML model performance. However, data  
785 augmentation and incorporating physics knowledge, e.g., physical laws, nominal material  
786 properties/behaviors, are expected to mitigate such issue for stages of manufacturing, testing  
787 and monitoring. With the aid of physical laws, AI/ML algorithms have the potential to  
788 comprehend material behaviors with unseen configurations, e.g., fraction of fibers, and  
789 predict “A-Basis” and “B-Basis” values for FRP composite design when trained on a  
790 moderate size dataset. In summary, techniques such as data augmentation, physics-informed  
791 machine learning and weakly-supervised learning are available to alleviate data issues, but it  
792 remains to be an open question waiting for further exploration.

793 **7.2.2 Other Issues and Potential Solutions**

794 In addition to data issues, other issues of AI/ML methods such as explainability and  
795 interpretability, uncertainty quantification, computational cost, and data privacy are discussed  
796 as follows.

797 (1) Since data-driven methods such as AI/ML models are usually regarded as black-box  
798 procedures, the interpretability and explainability of AI/ML models and results have

attracted much research interest, which are also a major drawback especially when an analysis and interpretation of model are desirable which physically makes sense in an engineering application. To address this and facilitate the implementation of black-box models, explainable AI (XAI) that allows users to comprehend results produced by AI/ML algorithms should be investigated to associate with engineering knowledge.

(2) Compared to classic statistical methods, it is more difficult to analyze uncertainty propagation and perform uncertainty quantification in AI/ML, especially DL, models. Uncertainty quantification is significant in considering safety and reliability in any engineering problems. GPR as a cheap-to-evaluate AI/ML model with the capability of uncertainty analysis has been widely used in the field of FRP composites. However, it is not typically utilized for the out-of-distribution (OOD) samples [222], i.e., unseen samples, which are specially interested in the engineering design. Even with more advanced AI/ML models such as Bayesian neural networks and deterministic methods, uncertainty quantification of AI/ML results in high-performance composites is limited and needs more investigation.

(3) One of the practical issues in the implementation of AI/ML methods is the requirement of large amounts of computational resources and time especially for those large-scale models with much data. The computational cost of AI/ML models poses challenges for the extension to large scales and integration with legacy manufacturing systems.

(4) Considering the complexity of high-performance FRP composites such as anisotropy, inhomogeneity, inherent large variability, human factor, etc., adopting AI/ML methods requires more dedicated and special design and more data to ensure the model capture the underlying complicated physics and patterns. End-to-end modeling of the multi-stage manufacturing process of composites using AI/ML techniques remains under-explored.

(5) Regarding safety-critical applications such as aerospace industry, adopting data-extensive

824 AI/ML models for each stage of high-performance FRP composite cycle life will require  
825 additional attention to data privacy concerns and regulatory compliance. While the former  
826 one can be addressed by techniques such as federated learning which is a collaboratively  
827 decentralized privacy-preserving ML scheme to overcome challenges of data silos [223]  
828 and often applied to privacy-sensitive areas such as healthcare, the latter concern requires  
829 a much more cautious design of AI/ML algorithms with appropriate constraints to comply  
830 with aerospace regulations.

831

### 832 **7.3 Future Research Directions**

833 Despite of these great advancements and extensive efforts in adopting AI/ML models for  
834 engineering problems of high-performance FRP composite structures, there are still some  
835 possible future research directions in certain areas that are presented below to provide a clear  
836 and systematic overview of current challenges and outlooks in this field.

#### 837 **7.3.1 Exploring and Exploiting Generative Models**

838 There are gaps in designing FRP composite structures based on AI/ML models. The  
839 complex material structure and multiple-material system make it challenging to fully  
840 understand the relationship between design space and material response merely relying on  
841 physical knowledge. In the general framework of material inverse design, VAE is able to  
842 learn a stable material representation in the low-dimensional subspace and the decoder  
843 produces structures towards the targeted material property when combined with a generative  
844 process and predictive model that links to material responses. Novel AI/ML models,  
845 especially generative models, have great potential to help design and develop new materials,  
846 as demonstrated in [116] where such method has been applied to the crystal materials. When  
847 considering FRP composites, a potential direction is to explore structures and/or  
848 combinations of fiber and matrix that are more resilient and robust to curing PIDs through the

849 way of inverse design with the aid of generative AI/ML models.

### 850 **7.3.2 Incorporating Physics and Engineering Knowledge**

851 PIML and PINN generally perform better when solving engineering problems that are  
852 related to nonlinear ODEs/PDEs via incorporating physics knowledge into ML and NN  
853 frameworks. Such models are suitable for modeling of continuous processes such as  
854 manufacturing, curing, and testing processes of composite structures. Based on prior domain  
855 knowledge, multiple ways of integrating physics knowledge can be selected when building  
856 PIML/PINN models such as adding physics-informed terms that are related to the  
857 initial/boundary conditions to loss function, choosing activation functions based on physical  
858 rationale, incorporating known or partially known ODEs/PDEs into NN structures, etc. In  
859 addition, some advanced PIML/PINN models such as physics-informed neural operators  
860 (PINOs) [224-226], Neural ODEs [227], etc. can either map between the input-output space  
861 continuously or construct a continuous-depth structure, improving extrapolation performance.  
862 This is valuable to some engineering problem where limited experiment data cannot fully  
863 cover the input space, which applies to the field of FRP composites. Therefore, hybrid  
864 physics-based and data-driven approaches provide opportunities to better understand and  
865 model the manufacturing and testing processes of FRP composite structures.

### 866 **7.3.3 Addressing High-Dimensional and Heterogeneous Data**

867 Considering the high-dimensional data in NDI on composites such as C-scan data from  
868 UT and a time-series of image signals, e.g., DIC, thermography, shearography, etc., it is  
869 important to process the whole-field spatiotemporal data that is usually in the form of 3-order  
870 tensor, whereas most of current works extract features through dimension reduction methods  
871 such as PCA, inevitably losing information to some extent. Tensor-based data analytics such  
872 as tensor decomposition and tensor-based network can play a role in processing such high-  
873 dimensional data by preserving and leveraging the tensor structure and embedded

874 spatiotemporal information, which can also be applied to the scenarios where multiple  
875 sensors are distributed and deployed in SHM by fusing sensor signals together. Another  
876 potential approach to deal with multiple distributed sensor signals is multi-model method.  
877 Meta-learning, which learns from a collection of similar tasks with the goal of generalization  
878 and adaptation to a related but new task [228], has the potential to be applied to multiple  
879 homogeneous sensors. On the other hand, the SHM with heterogeneous sensor setting is  
880 expected to be benefited from multi-model meta-learning techniques [229, 230].

#### 881 **7.3.4 End-to-End and Calibration-Free Modeling**

882 Modeling an engineering problem such as FRP composite structures often involves a  
883 calibration process on some parameters, e.g., material properties, which are usually unknown  
884 and intrinsic property of material. Such parameters vary among different materials yet are  
885 constants during manufacturing for each material. Conventional methods for calibration rely  
886 on laborious tests that are expensive and time-consuming. An end-to-end modeling is  
887 expected to bypass the calibration process of material properties as these properties are also  
888 the result of manufacturing parameters. With the aid of AI/ML methods, especially those  
889 advanced models such as PINN, etc., complex nonlinearities in the relationship between  
890 manufacturing and material response are possible to be revealed. On the other hand,  
891 calibration-free algorithm [231] is potential to be applied on continuous processes with  
892 multiple sensors, e.g., SHM, to “cancelling out” calibration parameters with an appropriate  
893 design.

#### 894 **7.3.5 Multiscale Process Modeling**

895 Multiscale modeling of structural composites for the mechanical performance analysis  
896 has been explored in the past through numerical simulations, which often follows the process  
897 where one first computes properties of one entity such as individual plies at a small length  
898 scale, then homogenizes into a constitutive model and passes to the next level of length scale

899 to estimate the corresponding behavior of a larger entity, e.g., composite laminate, and repeat  
900 to the level of structural component afterwards [232]. A local-to-global multiscale simulation  
901 strategy composed of computational micromechanics for ply level [233], mesomechanics for  
902 laminate level [234], and mechanics for component level [235], however, requires multiple  
903 runs of time-consuming numerical simulations. On the other hand, AI/ML methods are being  
904 utilized to learn the physics at different length scales and to substitute simulations to improve  
905 the efficiency of multiscale analysis of FRP composite structures [55, 236-239]. Generally,  
906 AI/ML methods such as MultiScaleGNN [240] serve as surrogate models of numerical ones  
907 to reduce simulation efforts in the inference stage and the PINN framework is employed to  
908 strengthen the learning capabilities. As a promising alternative for traditional physics-based  
909 numerical simulation, AI/ML techniques for the multiscale process modeling can be further  
910 improved in the aspects of smoother transition between scales and more robust prediction.

911

## 912 **Acknowledgements**

913 This material is based upon work supported by the National Science Foundation (NSF) under  
914 Grant EEC-2052714. The authors acknowledge the generous support from NSF and member  
915 companies of the Composite and Hybrid Materials Interfacing (CHMI) IUCRC.

916

## 917 **References**

918 [1] Butler KT, Davies DW, Cartwright H, Isayev O, Walsh A. Machine learning for  
919 molecular and materials science. *Nature* 2018;559(7715):547-55.  
920 [2] Clyne TW, Hull D. *An Introduction to Composite Materials*: Cambridge university press;  
921 2019.

922 [3] Waqar T, Akhtar SS, Arif AFM, Hakeem AS. Design and development of ceramic-based  
923 composites with tailored properties for cutting tool inserts. *Ceram Int*  
924 2018;44(18):22421-31.

925 [4] Zhang X, Yang W, Wang Q, Huang F, Gao C, Xue L. Tuning the nano-porosity and  
926 nano-morphology of nano-filtration (NF) membranes: Divalent metal nitrates  
927 modulated inter-facial polymerization. *J Membr Sci* 2021;640:119780.

928 [5] Kubota M, Hayakawa K, Todoroki A. Effect of build-up orientations and process  
929 parameters on the tensile strength of 3D printed short carbon fiber/PA-6 composites.  
930 *Adv Compos Mater* 2022;31(2):119-36.

931 [6] McIlhagger A, Archer E, McIlhagger R. Manufacturing processes for composite materials  
932 and components for aerospace applications. In: *Polymer Composites in the Aerospace*  
933 *Industry*: Elsevier; 2020. p. 59-81.

934 [7] Tiwary A, Kumar R, Chohan JS. A review on characteristics of composite and advanced  
935 materials used for aerospace applications. *Mater Today Proc* 2022;51:865-70.

936 [8] Davies G, Hitchings D, Ankersen J. Predicting delamination and debonding in modern  
937 aerospace composite structures. *Compos Sci Technol* 2006;66(6):846-54.

938 [9] Meola C, Boccardi S, Carlomagno GM. Composite material overview and its testing for  
939 aerospace components. In: *Sustainable Composites for Aerospace Applications*:  
940 Elsevier; 2018. p. 69-108.

941 [10] Henning F, Kärger L, Dörr D, Schirmaier FJ, Seuffert J, Bernath A. Fast processing and  
942 continuous simulation of automotive structural composite components. *Compos Sci*  
943 *Technol* 2019;171:261-79.

944 [11] Rajak DK, Pagar D, Behera A, Menezes PL. Role of composite materials in automotive  
945 sector: potential applications. In: *Advances in Engine Tribology* 2022. p. 193-217.

946 [12] Rubino F, Nisticò A, Tucci F, Carbone P. Marine application of fiber reinforced  
947 composites: a review. *J Mar Sci Eng* 2020;8(1):26.

948 [13] Goudarzi RH, Khedmati MR. An experimental and numerical investigation of adhesive  
949 bond strength in Al-GFRP single lap and double butt lap joints due to applied  
950 longitudinal loads. *Ships Offshore Struct* 2020;15(4):403-16.

951 [14] Wu W-H, Young W-B. Structural analysis and design of the composite wind turbine  
952 blade. *Appl Compos Mater* 2012;19:247-57.

953 [15] Murray RE, Beach R, Barnes D, Snowberg D, Berry D, Rooney S, et al. Structural  
954 validation of a thermoplastic composite wind turbine blade with comparison to a  
955 thermoset composite blade. *Renew Energy* 2021;164:1100-7.

956 [16] Prashanth S, Subbaya K, Nithin K, Sachidananda S. Fiber reinforced composites-a  
957 review. *J Mater Sci Eng* 2017;6(03):2-6.

958 [17] National Research Council, Division on Engineering Physical Sciences, National  
959 Materials Advisory Board, Committee on Durability Life Prediction of Polymer Matrix  
960 Composites in Extreme Environments. *Going to Extremes: Meeting the Emerging  
961 Demand for Durable Polymer Matrix Composites*: National Academies Press; 2005.

962 [18] Kesarwani S. Polymer composites in aviation sector. *Int J Eng Res* 2017;6(10).

963 [19] Mortazavian S, Fatemi A. Effects of fiber orientation and anisotropy on tensile strength  
964 and elastic modulus of short fiber reinforced polymer composites. *Compos B Eng*  
965 2015;72:116-29.

966 [20] Owens JF, Lee-Sullivan P. Stiffness behaviour due to fracture in adhesively bonded  
967 composite-to-aluminum joints I. Theoretical model. *Int J Adhes Adhes* 2000;20(1):39-  
968 45.

969 [21] Deb A, Malvade I, Biswas P, Schroeder J. An experimental and analytical study of the  
970 mechanical behaviour of adhesively bonded joints for variable extension rates and  
971 temperatures. *Int J Adhes Adhes* 2008;28(1-2):1-15.

972 [22] Anandan S, Dhaliwal G, Huo Z, Chandrashekara K, Apetre N, Iyyer N. Curing of thick  
973 thermoset composite laminates: multiphysics modeling and experiments. *Appl Compos  
974 Mater* 2018;25:1155-68.

975 [23] Zimmermann J, Schalm T, Sadeghi M, Gabener A, Schröder K-U. Analytical stiffness  
976 analysis of adhesively bonded single-lap joints subjected to out-of-plane deflection due  
977 to tensile loading. *J Adhes* 2022;98(11):1635-62.

978 [24] Campilho RD, Banea MD, Neto J, da Silva LF. Modelling adhesive joints with cohesive  
979 zone models: effect of the cohesive law shape of the adhesive layer. *Int J Adhes Adhes*  
980 2013;44:48-56.

981 [25] Rao GVG, Mahajan P, Bhatnagar N. Machining of UD-GFRP composites chip  
982 formation mechanism. *Compos Sci Technol* 2007;67(11-12):2271-81.

983 [26] Tan W, Naya F, Yang L, Chang T, Falzon B, Zhan L, et al. The role of interfacial  
984 properties on the intralaminar and interlaminar damage behaviour of unidirectional  
985 composite laminates: Experimental characterization and multiscale modelling. *Compos  
986 B Eng* 2018;138:206-21.

987 [27] Mendoza A, Schneider J, Parra E, Roux S. The correlation framework: Bridging the gap  
988 between modeling and analysis for 3D woven composites. *Compos Struct*  
989 2019;229:111468.

990 [28] Bamane SS, Gaikwad PS, Radue MS, Gowtham S, Odegard GM. Wetting simulations of  
991 high-performance polymer resins on carbon surfaces as a function of temperature using  
992 molecular dynamics. *Polymers* 2021;13(13):2162.

993 [29] Deshpande PP, Radue MS, Gaikwad P, Bamane S, Patil SU, Pisani WA, et al. Prediction  
994 of the interfacial properties of high-performance polymers and flattened CNT-  
995 reinforced composites using molecular dynamics. *Langmuir* 2021;37(39):11526-34.

996 [30] Lin K, Wang Z. Multiscale mechanics and molecular dynamics simulations of the  
997 durability of fiber-reinforced polymer composites. *Commun Mater* 2023;4(1):66.

998 [31] Bamane SS, Jakubinek MB, Kanhaiya K, Ashrafi B, Heinz H, Odegard GM. Boron  
999 nitride nanotubes: force field parameterization, epoxy interactions, and comparison  
1000 with carbon nanotubes for high-performance composite materials. *ACS Appl Nano  
1001 Mater* 2023;6(5):3513-24.

1002 [32] Fleischer J, Teti R, Lanza G, Mativenga P, Möhring H-C, Caggiano A. Composite  
1003 materials parts manufacturing. *CIRP Ann Manuf Technol* 2018;67(2):603-26.

1004 [33] Yuan Z, Kong L, Gao D, Tong X, Feng Y, Yang G, et al. Multi-objective approach to  
1005 optimize cure process for thick composite based on multi-field coupled model with  
1006 RBF surrogate model. *Compos Commun* 2021;24:100671.

1007 [34] Cristiani D, Sbarufatti C, Giglio M. Damage diagnosis and prognosis in composite  
1008 double cantilever beam coupons by particle filtering and surrogate modelling. *Struct  
1009 Health Monit* 2021;20(3):1030-50.

1010 [35] Cristiani D, Sbarufatti C, Cadini F, Giglio M. Fatigue damage diagnosis and prognosis  
1011 of an aeronautical structure based on surrogate modelling and particle filter. *Struct  
1012 Health Monit* 2021;20(5):2726-46.

1013 [36] Carbone P, Aleksendrić D, Ćirović V, Palazzo GS. Meta-modeling of the curing process  
1014 of thermoset matrix composites by means of a FEM-ANN approach. *Compos B Eng*  
1015 2014;67:441-8.

1016 [37] Niaki SA, Haghigat E, Campbell T, Poursartip A, Vaziri R. Physics-informed neural  
1017 network for modelling the thermochemical curing process of composite-tool systems  
1018 during manufacture. *Comput Methods Appl Mech Eng* 2021;384:113959.

1019 [38] Hui X, Xu Y, Zhang W, Zhang W. Cure process evaluation of CFRP composites via  
1020 neural network: From cure kinetics to thermochemical coupling. *Compos Struct*  
1021 2022;288:115341.

1022 [39] Wang S, Xu Z, Stratford T, Li B, Zeng Q, Su J. Machine learning approach for analysing  
1023 and predicting the modulus response of the structural epoxy adhesive at elevated  
1024 temperatures. *J Adhes* 2023;1-19.

1025 [40] Liu C, He Q, Zhao A, Wu T, Song Z, Liu B, et al. Operator Learning for Predicting  
1026 Mechanical Response of Hierarchical Composites with Applications of Inverse Design.  
1027 *Int J Appl Mech* 2023;15(04):2350028.

1028 [41] Shokrollahi Y, Nikahd MM, Gholami K, Azamirad G. Deep Learning Techniques for  
1029 Predicting Stress Fields in Composite Materials: A Superior Alternative to Finite  
1030 Element Analysis. *J Compos Sci* 2023;7(8):311.

1031 [42] Mital SK, Arnold SM, Murthy PL, Hearley BL. Prediction of Stiffness and Fatigue  
1032 Lives of Polymer Matrix Composite Laminates Using Artificial Neural Networks.  
1033 2023.

1034 [43] Samaitis V, Yilmaz B, Jasiuniene E. Adhesive bond quality classification using machine  
1035 learning algorithms based on ultrasonic pulse-echo immersion data. *J Sound Vib*  
1036 2023;546:117457.

1037 [44] Diaz-Escobar J, Díaz-Montiel P, Venkataraman S, Díaz-Ramírez A. Classification and  
1038 characterization of damage in composite laminates using electrical resistance  
1039 tomography and supervised machine learning. *Struct Control Health Monit* 2023;2023.

1040 [45] Schmidt C, Hocke T, Denkena B. Deep learning-based classification of production  
1041 defects in automated-fiber-placement processes. *Prod Eng* 2019;13:501-9.

1042 [46] Du J, Yue X, Hunt JH, Shi J. Optimal placement of actuators via sparse learning for  
1043 composite fuselage shape control. *J Manuf Sci Eng* 2019;141(10):101004.

1044 [47] Du J, Cao S, Hunt JH, Huo X, Shi J. A new sparse-learning model for maximum gap  
1045 reduction of composite fuselage assembly. *Technometrics* 2022;64(3):409-18.

1046 [48] Zhong Z, Mou S, Hunt JH, Shi J. Finite Element Analysis Model-Based Cautious  
1047 Automatic Optimal Shape Control for Fuselage Assembly. *J Manuf Sci Eng*  
1048 2022;144(8):081009.

1049 [49] Carbas RJ, Palmares MP, da Silva LF. Experimental and FE study of hybrid laminates  
1050 aluminium carbon-fibre joints with different lay-up configurations. *Manuf Rev*  
1051 2020;7:2.

1052 [50] Ye J, Yan Y, Li J, Hong Y, Tian Z. 3D explicit finite element analysis of tensile failure  
1053 behavior in adhesive-bonded composite single-lap joints. *Compos Struct*  
1054 2018;201:261-75.

1055 [51] Kang H, Lee JH, Choe Y, Lee SG. Prediction of lap shear strength and impact peel  
1056 strength of epoxy adhesive by machine learning approach. *Nanomaterials*  
1057 2021;11(4):872.

1058 [52] Wang Q, Jackson JA, Ge Q, Hopkins JB, Spadaccini CM, Fang NX. Lightweight  
1059 mechanical metamaterials with tunable negative thermal expansion. *Phys Rev Lett*  
1060 2016;117(17):175901.

1061 [53] Luo L, Zhang B, Zhang G, Li X, Fang X, Li W, et al. Rapid prediction and inverse  
1062 design of distortion behaviors of composite materials using artificial neural networks.  
1063 *Polym Adv Technol* 2021;32(3):1049-60.

1064 [54] Meister S, Wermes MA, Stüve J, Groves RM. Review of image segmentation techniques  
1065 for layup defect detection in the Automated Fiber Placement process: A comprehensive  
1066 study to improve AFP inspection. *J Intell Manuf* 2021;32(8):2099-119.

1067 [55] Gupta A, Bhaduri A, Graham-Brady L. Accelerated multiscale mechanics modeling in a  
1068 deep learning framework. *Mech Mater* 2023;104709.

1069 [56] Tao C, Zhang C, Ji H, Qiu J. Application of neural network to model stiffness  
1070 degradation for composite laminates under cyclic loadings. *Compos Sci Technol*  
1071 2021;203:108573.

1072 [57] Ewald V, Groves RM, Benedictus R. DeepSHM: A deep learning approach for structural  
1073 health monitoring based on guided Lamb wave technique. In: *Proceedings of Sensors*  
1074 and *Smart Structures Technologies for Civil, Mechanical, and Aerospace Systems*  
1075 2019. 2019. p. 84-99.

1076 [58] Luan C, Yao X, Zhang C, Fu J, Wang B. Integrated self-monitoring and self-healing  
1077 continuous carbon fiber reinforced thermoplastic structures using dual-material three-  
1078 dimensional printing technology. *Compos Sci Technol* 2020;188:107986.

1079 [59] Ertel W. *Introduction to Artificial Intelligence*: Springer; 2018.

1080 [60] Boden MA. *Artificial Intelligence: A Very Short Introduction*: Oxford University Press;  
1081 2018.

1082 [61] Mahesh B. Machine learning algorithms-a review. *Int J Sci Res* 2020;9(1):381-6.

1083 [62] McCulloch WS, Pitts W. A logical calculus of the ideas immanent in nervous activity.  
1084 *Bull Math biophys* 1943;5:115-33.

1085 [63] Rosenblatt F. The perceptron: a probabilistic model for information storage and  
1086 organization in the brain. *Psychol Rev* 1958;65(6):386.

1087 [64] Rosenblatt F. *Principles of Neurodynamics: Perceptrons and the Theory of Brain*  
1088 *Mechanisms*. Washington, DC: Spartan books 1962.

1089 [65] Rumelhart DE, Hinton GE, Williams RJ. Learning representations by back-propagating  
1090 errors. *Nature* 1986;323(6088):533-6.

1091 [66] LeCun Y, Boser B, Denker JS, Henderson D, Howard RE, Hubbard W, et al.  
1092 Backpropagation applied to handwritten zip code recognition. *Neural Comput*  
1093 1989;1(4):541-51.

1094 [67] LeCun Y, Bottou L, Bengio Y, Haffner P. Gradient-based learning applied to document  
1095 recognition. *Proc IEEE* 1998;86(11):2278-324.

1096 [68] Boser BE, Guyon IM, Vapnik VN. A training algorithm for optimal margin classifiers.  
1097 In: *Proceedings of the Fifth Annual Workshop on Computational Learning Theory*  
1098 (COLT). 1992. p. 144-52.

1099 [69] Cortes C, Vapnik V. Support-vector networks. *Mach Learn* 1995;20:273-97.

1100 [70] Keller JM, Gray MR, Givens JA. A fuzzy k-nearest neighbor algorithm. *IEEE Trans*  
1101 *Syst Man Cybern Syst* 1985(4):580-5.

1102 [71] Hochreiter S, Schmidhuber J. Long short-term memory. *Neural Comput* 1997;9(8):1735-  
1103 80.

1104 [72] Settles B. Active learning literature survey. 2009.

1105 [73] LeCun Y, Bengio Y, Hinton G. Deep learning. *Nature* 2015;521(7553):436-44.

1106 [74] Karniadakis GE, Kevrekidis IG, Lu L, Perdikaris P, Wang S, Yang L. Physics-informed  
1107 machine learning. *Nat Rev Phys* 2021;3(6):422-40.

1108 [75] Hospedales T, Antoniou A, Micaelli P, Storkey A. Meta-learning in neural networks: A  
1109 survey. *IEEE PAMI* 2021;44(9):5149-69.

1110 [76] van de Ven GM, Tuytelaars T, Tolias AS. Three types of incremental learning. *Nat*  
1111 *Mach Intell* 2022;4(12):1185-97.

1112 [77] Krizhevsky A, Sutskever I, Hinton GE. Imagenet classification with deep convolutional  
1113 neural networks. *Adv Neural Inf Process Syst* 2012;25.

1114 [78] He K, Zhang X, Ren S, Sun J. Deep residual learning for image recognition. In:  
1115 Proceedings of the IEEE Conference on Computer Vision and Pattern Recognition  
1116 (CVPR). 2016. p. 770-8.

1117 [79] Girshick R, Donahue J, Darrell T, Malik J. Region-based convolutional networks for  
1118 accurate object detection and segmentation. IEEE PAMI 2015;38(1):142-58.

1119 [80] Girshick R. Fast r-cnn. In: Proceedings of the IEEE International Conference on  
1120 Computer Vision (ICCV). 2015. p. 1440-8.

1121 [81] Ren S, He K, Girshick R, Sun J. Faster r-cnn: Towards real-time object detection with  
1122 region proposal networks. Adv Neural Inf Process Syst 2015;28.

1123 [82] He K, Gkioxari G, Dollár P, Girshick R. Mask r-cnn. In: Proceedings of the IEEE  
1124 International Conference on Computer Vision (ICCV). 2017. p. 2961-9.

1125 [83] Elman JL. Finding structure in time. Cogn Sci 1990;14(2):179-211.

1126 [84] Schuster M, Paliwal KK. Bidirectional recurrent neural networks. IEEE Trans Signal  
1127 Process 1997;45(11):2673-81.

1128 [85] Pascanu R, Gulcehre C, Cho K, Bengio Y. How to construct deep recurrent neural  
1129 networks. In: Proceedings of the Second International Conference on Learning  
1130 Representations (ICLR). 2014.

1131 [86] Goodfellow I, Pouget-Abadie J, Mirza M, Xu B, Warde-Farley D, Ozair S, et al.  
1132 Generative adversarial nets. Adv Neural Inf Process Syst 2014;27.

1133 [87] Denton EL, Chintala S, Fergus R. Deep generative image models using a laplacian  
1134 pyramid of adversarial networks. Adv Neural Inf Process Syst 2015;28.

1135 [88] Chen X, Duan Y, Houthooft R, Schulman J, Sutskever I, Abbeel P. Infogan:  
1136 Interpretable representation learning by information maximizing generative adversarial  
1137 nets. Adv Neural Inf Process Syst 2016;29.

1138 [89] Vaswani A, Shazeer N, Parmar N, Uszkoreit J, Jones L, Gomez AN, et al. Attention is  
1139 all you need. *Adv Neural Inf Process Syst* 2017;30.

1140 [90] Fukui H, Hirakawa T, Yamashita T, Fujiyoshi H. Attention branch network: Learning of  
1141 attention mechanism for visual explanation. In: *Proceedings of the IEEE/CVF*  
1142 *Conference on Computer Vision and Pattern Recognition (CVPR)*. 2019. p. 10705-14.

1143 [91] Raissi M, Perdikaris P, Karniadakis GE. Physics-informed neural networks: A deep  
1144 learning framework for solving forward and inverse problems involving nonlinear  
1145 partial differential equations. *J Comput Phys* 2019;378:686-707.

1146 [92] Gozalo-Brizuela R, Garrido-Merchan EC. ChatGPT is not all you need. A State of the  
1147 Art Review of large Generative AI models. *arXiv preprint arXiv:230104655* 2023.

1148 [93] Frank M, Drikakis D, Charassis V. Machine-learning methods for computational science  
1149 and engineering. *Computation* 2020;8(1):15.

1150 [94] Sosso GC, Miceli G, Caravati S, Giberti F, Behler Jr, Bernasconi M. Fast crystallization  
1151 of the phase change compound GeTe by large-scale molecular dynamics simulations. *J*  
1152 *Phys Chem Lett* 2013;4(24):4241-6.

1153 [95] Gabardi S, Baldi E, Bosoni E, Campi D, Caravati S, Sosso G, et al. Atomistic  
1154 simulations of the crystallization and aging of GeTe nanowires. *J Phys Chem C*  
1155 2017;121(42):23827-38.

1156 [96] Milano M, Koumoutsakos P. Neural network modeling for near wall turbulent flow. *J*  
1157 *Comput Phys* 2002;182(1):1-26.

1158 [97] Chang FJ, Yang HC, Lu JY, Hong JH. Neural network modelling for mean velocity and  
1159 turbulence intensities of steep channel flows. *Hydrol Process Int J* 2008;22(2):265-74.

1160 [98] Ghaderi A, Morovati V, Dargazany R. A physics-informed assembly of feed-forward  
1161 neural network engines to predict inelasticity in cross-linked polymers. *Polymers*  
1162 2020;12(11):2628.

1163 [99] Yeh I-C. Modeling of strength of high-performance concrete using artificial neural  
1164 networks. *Cem Concr Res* 1998;28(12):1797-808.

1165 [100] Nanduri A, Sherry L. Anomaly detection in aircraft data using Recurrent Neural  
1166 Networks (RNN). In: Proceedings of the 2016 Integrated Communications Navigation  
1167 and Surveillance (ICNS). 2016. p. 5C2-1-5C2-8.

1168 [101] Smaoui N, Al-Enezi S. Modelling the dynamics of nonlinear partial differential  
1169 equations using neural networks. *J Comput Appl Math* 2004;170(1):27-58.

1170 [102] Pan S, Duraisamy K. Long-time predictive modeling of nonlinear dynamical systems  
1171 using neural networks. *Complexity* 2018;2018:1-26.

1172 [103] Akhare D, Luo T, Wang J-X. Physics-integrated neural differentiable (PiNDiff) model  
1173 for composites manufacturing. *Comput Methods Appl Mech Eng* 2023;406:115902.

1174 [104] Kashinath K, Mustafa M, Albert A, Wu J, Jiang C, Esmaeilzadeh S, et al. Physics-  
1175 informed machine learning: case studies for weather and climate modelling. *Philos  
1176 Trans R Soc A* 2021;379(2194):20200093.

1177 [105] Weber M, Kube S. Robust perron cluster analysis for various applications in  
1178 computational life science. In: Proceedings of International Symposium on  
1179 Computational Life Science. 2005. p. 57-66.

1180 [106] Wolf A, Kirschner KN. Principal component and clustering analysis on molecular  
1181 dynamics data of the ribosomal L11· 23S subdomain. *J Mol Model* 2013;19:539-49.

1182 [107] Decherchi S, Berteotti A, Bottegoni G, Rocchia W, Cavalli A. The ligand binding  
1183 mechanism to purine nucleoside phosphorylase elucidated via molecular dynamics and  
1184 machine learning. *Nat Commun* 2015;6(1):6155.

1185 [108] Zhou J, Troyanskaya OG. Predicting effects of noncoding variants with deep learning-  
1186 based sequence model. *Nat Methods* 2015;12(10):931-4.

1187 [109] Nguyen NG, Tran VA, Phan D, Lumbanraja FR, Faisal MR, Abapihi B, et al. DNA  
1188 sequence classification by convolutional neural network. *J Biomed Sci Eng*  
1189 2016;9(5):280-6.

1190 [110] Boll B, Willmann E, Fiedler B, Meißner RH. Weak adhesion detection—enhancing the  
1191 analysis of vibroacoustic modulation by machine learning. *Compos Struct*  
1192 2021;273:114233.

1193 [111] Tao F, Liu X, Du H, Tian S, Yu W. Discover failure criteria of composites from  
1194 experimental data by sparse regression. *Compos B Eng* 2022;239:109947.

1195 [112] Tao C, Zhang C, Ji H, Qiu J. Fatigue damage characterization for composite laminates  
1196 using deep learning and laser ultrasonic. *Compos B Eng* 2021;216:108816.

1197 [113] Freed Y, Salviato M, Zobeiry N. Implementation of a probabilistic machine learning  
1198 strategy for failure predictions of adhesively bonded joints using cohesive zone  
1199 modeling. *Int J Adhes Adhes* 2022;118:103226.

1200 [114] Pasquet J, Bertin E, Treyer M, Arnouts S, Fouchez D. Photometric redshifts from  
1201 SDSS images using a convolutional neural network. *Astron Astrophys* 2019;621:A26.

1202 [115] Narayanan BN, Djaneye-Boundjou O, Kebede TM. Performance analysis of machine  
1203 learning and pattern recognition algorithms for malware classification. In: Proceedings  
1204 of 2016 IEEE National Aerospace and Electronics Conference (NAECON) and Ohio  
1205 Innovation Summit (OIS). 2016. p. 338-42.

1206 [116] Xie T, Fu X, Ganea O-E, Barzilay R, Jaakkola TS. Crystal Diffusion Variational  
1207 Autoencoder for Periodic Material Generation. International Conference on Learning  
1208 Representations (ICLR)2021.

1209 [117] Lyngby P, Thygesen KS. Data-driven discovery of 2D materials by deep generative  
1210 models. *Npj Comput Mater* 2022;8(1):232.

1211 [118] Nosengo N. The material code. *Nature* 2016;533(7601):22-5.

1212 [119] de Pablo JJ, Jackson NE, Webb MA, Chen L-Q, Moore JE, Morgan D, et al. New  
1213 frontiers for the materials genome initiative. *Npj Comput Mater* 2019;5(1):41.

1214 [120] Gómez-Bombarelli R, Aguilera-Iparraguirre J, Hirzel TD, Duvenaud D, Maclaurin D,  
1215 Blood-Forsythe MA, et al. Design of efficient molecular organic light-emitting diodes  
1216 by a high-throughput virtual screening and experimental approach. *Nat Mater*  
1217 2016;15(10):1120-7.

1218 [121] Liu Y, Zhang J, Zhang Y, Yoon HY, Jia X, Roman M, et al. Accelerated Engineering  
1219 of Optimized Functional Composite Hydrogels via High-Throughput Experimentation.  
1220 *ACS Appl Mater Interfaces* 2023.

1221 [122] Wei J, Chu X, Sun XY, Xu K, Deng HX, Chen J, et al. Machine learning in materials  
1222 science. *InfoMat* 2019;1(3):338-58.

1223 [123] Kim K, Kang S, Yoo J, Kwon Y, Nam Y, Lee D, et al. Deep-learning-based inverse  
1224 design model for intelligent discovery of organic molecules. *Npj Comput Mater*  
1225 2018;4(1):67.

1226 [124] Nomura T, Kawamoto A, Kondoh T, Dede EM, Lee J, Song Y, et al. Inverse design of  
1227 structure and fiber orientation by means of topology optimization with tensor field  
1228 variables. *Compos B Eng* 2019;176:107187.

1229 [125] Jung T, Lee J, Nomura T, Dede EM. Inverse design of three-dimensional fiber  
1230 reinforced composites with spatially-varying fiber size and orientation using multiscale  
1231 topology optimization. *Compos Struct* 2022;279:114768.

1232 [126] Song S, Wang Z, Cheng Y. The inverse design and optimization for composite  
1233 materials with random uncertainty. In: *Proceedings of Journal of Physics: Conference  
1234 Series*. 2021. p. 012051.

1235 [127] Zobeiry N, Humfeld KD. A physics-informed machine learning approach for solving  
1236 heat transfer equation in advanced manufacturing and engineering applications. Eng  
1237 Appl Artif Intell 2021;101:104232.

1238 [128] Rajak DK, Pagar DD, Menezes PL, Linul E. Fiber-reinforced polymer composites:  
1239 Manufacturing, properties, and applications. Polymers 2019;11(10):1667.

1240 [129] Zambal S, Heindl C, Eitzinger C, Scharinger J. End-to-end defect detection in  
1241 automated fiber placement based on artificially generated data. In: Proceedings of  
1242 Fourteenth International Conference on Quality Control by Artificial Vision. 2019. p.  
1243 371-8.

1244 [130] Sacco C, Radwan AB, Anderson A, Harik R, Gregory E. Machine learning in  
1245 composites manufacturing: A case study of Automated Fiber Placement inspection.  
1246 Compos Struct 2020;250:112514.

1247 [131] Meister S, Wermes M, Stüve J, Groves RM. Investigations on Explainable Artificial  
1248 Intelligence methods for the deep learning classification of fibre layup defect in the  
1249 automated composite manufacturing. Compos B Eng 2021;224:109160.

1250 [132] Islam F, Wanigasekara C, Rajan G, Swain A, Prusty BG. An approach for process  
1251 optimisation of the Automated Fibre Placement (AFP) based thermoplastic composites  
1252 manufacturing using Machine Learning, photonic sensing and thermo-mechanics  
1253 modelling. Manuf Lett 2022;32:10-4.

1254 [133] Yuan S, Li S, Zhu J, Tang Y. Additive manufacturing of polymeric composites from  
1255 material processing to structural design. Compos B Eng 2021;219:108903.

1256 [134] Yanamandra K, Chen GL, Xu X, Mac G, Gupta N. Reverse engineering of additive  
1257 manufactured composite part by toolpath reconstruction using imaging and machine  
1258 learning. Compos Sci Technol 2020;198:108318.

1259 [135] Hu C, Hau WNJ, Chen W, Qin Q-H. The fabrication of long carbon fiber reinforced  
1260 polylactic acid composites via fused deposition modelling: Experimental analysis and  
1261 machine learning. *J Compos Mater* 2021;55(11):1459-72.

1262 [136] Wright WJ, Darville J, Celik N, Koerner H, Celik E. In-situ optimization of thermoset  
1263 composite additive manufacturing via deep learning and computer vision. *Addit Manuf*  
1264 2022;58:102985.

1265 [137] Lu L, Hou J, Yuan S, Yao X, Li Y, Zhu J. Deep learning-assisted real-time defect  
1266 detection and closed-loop adjustment for additive manufacturing of continuous fiber-  
1267 reinforced polymer composites. *Robot Comput Integr Manuf* 2023;79:102431.

1268 [138] Zhang C, Zhang G, Xu J, Shi XP, Wang X. Review of curing deformation control  
1269 methods for carbon fiber reinforced resin composites. *Polym Compos*  
1270 2022;43(6):3350-70.

1271 [139] Wang B, Fan S, Chen J, Yang W, Liu W, Li Y. A review on prediction and control of  
1272 curing process-induced deformation of continuous fiber-reinforced thermosetting  
1273 composite structures. *Compos A Appl Sci Manuf* 2023;165:107321.

1274 [140] Bezerra E, Bento M, Rocco J, Iha K, Lourenço V, Pardini L. Artificial neural network  
1275 (ANN) prediction of kinetic parameters of (CRFC) composites. *Comput Mater Sci*  
1276 2008;44(2):656-63.

1277 [141] Bheemreddy V, Huo Z, Chandrashekara K, Brack R. Modeling and simulation of cure  
1278 kinetics and flow in cavity-molded composites. *J Am Helicopter Soc* 2016;61(2):1-10.

1279 [142] Kim M, Zobeiry N. Machine learning for reduced-order modeling of composites  
1280 processing. In: Proceedings of the SAMPE Virtual Conference. 2021.

1281 [143] Zobeiry N, Poursartip A. Theory-guided machine learning for process simulation of  
1282 advanced composites. *arXiv preprint arXiv:210316010* 2021.

1283 [144] Jahromi PE, Shojaei A, Reza Pishvaie SM. Prediction and optimization of cure cycle of  
1284 thick fiber-reinforced composite parts using dynamic artificial neural networks. *J Reinforced  
1285 Plastics and Composites* 2012;31(18):1201-15.

1286 [145] Struzziero G, Teuwen JJ. A fully coupled thermo-mechanical analysis for the  
1287 minimisation of spring-in and process time in ultra-thick components for wind turbine  
1288 blades. *Composites A: Applied Science and Manufacture* 2020;139:106105.

1289 [146] Humfeld KD, Zobeiry N. Machine learning-based process simulation approach for real-  
1290 time optimization and active control of composites autoclave processing. In:  
1291 *Proceedings of the SAMPE Virtual Conference*. 2021.

1292 [147] Tang W, Xu Y, Hui X, Zhang W. Multi-objective optimization of curing profile for  
1293 autoclave processed composites: Simultaneous control of curing time and process-  
1294 induced defects. *Polymers* 2022;14(14):2815.

1295 [148] Kibrete F, Trzepieciński T, Gebremedhen HS, Woldemichael DE. Artificial  
1296 intelligence in predicting mechanical properties of composite materials. *J Composites Science*  
1297 2023;7(9):364.

1298 [149] Rashid MM, Pittie T, Chakraborty S, Krishnan NA. Learning the stress-strain fields in  
1299 digital composites using Fourier neural operator. *Iscience* 2022;25(11).

1300 [150] Bhaduri A, Gupta A, Graham-Brady L. Stress field prediction in fiber-reinforced  
1301 composite materials using a deep learning approach. *Composites B: Engineering* 2022;238:109879.

1302 [151] Khorrami MS, Mianroodi JR, Siboni NH, Goyal P, Svendsen B, Benner P, et al. An  
1303 artificial neural network for surrogate modeling of stress fields in viscoplastic  
1304 polycrystalline materials. *Npj Computational Materials* 2023;9(1):37.

1305 [152] Rahman A, Deshpande P, Radue MS, Odegard GM, Gowtham S, Ghosh S, et al. A  
1306 machine learning framework for predicting the shear strength of carbon nanotube-

1307 polymer interfaces based on molecular dynamics simulation data. *Compos Sci Technol*  
1308 2021;207:108627.

1309 [153] Yadav U, Pathrudkar S, Ghosh S. Interpretable machine learning model for the  
1310 deformation of multiwalled carbon nanotubes. *Phys Rev B* 2021;103(3):035407.

1311 [154] Abuodeh OR, Abdalla JA, Hawileh RA. Prediction of shear strength and behavior of  
1312 RC beams strengthened with externally bonded FRP sheets using machine learning  
1313 techniques. *Compos Struct* 2020;234:111698.

1314 [155] Yin B, Liew K. Machine learning and materials informatics approaches for evaluating  
1315 the interfacial properties of fiber-reinforced composites. *Compos Struct*  
1316 2021;273:114328.

1317 [156] Li M, Zhang H, Li S, Zhu W, Ke Y. Machine learning and materials informatics  
1318 approaches for predicting transverse mechanical properties of unidirectional CFRP  
1319 composites with microvoids. *Mater Des* 2022;224:111340.

1320 [157] Olfatbakhsh T, Milani AS. A highly interpretable materials informatics approach for  
1321 predicting microstructure-property relationship in fabric composites. *Compos Sci*  
1322 *Technol* 2022;217:109080.

1323 [158] Cai R, Wang K, Wen W, Peng Y, Baniassadi M, Ahzi S. Application of machine  
1324 learning methods on dynamic strength analysis for additive manufactured  
1325 polypropylene-based composites. *Polym Test* 2022;110:107580.

1326 [159] Pruksawan S, Lambard G, Samitsu S, Sodeyama K, Naito M. Prediction and  
1327 optimization of epoxy adhesive strength from a small dataset through active learning.  
1328 *Sci Technol Adv Mater* 2019;20(1):1010-21.

1329 [160] Rangaswamy H, Sogalad I, Basavarajappa S, Acharya S, Manjunath Patel G.  
1330 Experimental analysis and prediction of strength of adhesive-bonded single-lap

1331 composite joints: Taguchi and artificial neural network approaches. *SN Appl Sci*  
1332 2020;2:1-15.

1333 [161] Gu Z, Liu Y, Hughes DJ, Ye J, Hou X. A parametric study of adhesive bonded joints  
1334 with composite material using black-box and grey-box machine learning methods:  
1335 Deep neuron networks and genetic programming. *Compos B Eng* 2021;217:108894.

1336 [162] Sharma S, Awasthi R, Sastry YS, Budarapu PR. Physics-informed neural networks for  
1337 estimating stress transfer mechanics in single lap joints. *J Zhejiang Univ Sci A*  
1338 2021;22(8):621-31.

1339 [163] Kaiser I, Richards N, Ogasawara T, Tan K. Machine learning algorithms for deeper  
1340 understanding and better design of composite adhesive joints. *Mater Today Commun*  
1341 2023;34:105428.

1342 [164] Mottaghian F, Taheri F. Machine learning/finite element analysis-A collaborative  
1343 approach for predicting the axial impact response of adhesively bonded joints with  
1344 unique sandwich composite adherends. *Compos Sci Technol* 2023;242:110162.

1345 [165] Sommer D, Haufe A, Middendorf P. A machine learning material model for structural  
1346 adhesives in finite element analysis. *Int J Adhes Adhes* 2022;117:103160.

1347 [166] Freed Y, Zobeiry N, Salviato M. Development of aviation industry-oriented  
1348 methodology for failure predictions of brittle bonded joints using probabilistic machine  
1349 learning. *Compos Struct* 2022;297:115979.

1350 [167] Su M, Zhong Q, Peng H, Li S. Selected machine learning approaches for predicting the  
1351 interfacial bond strength between FRPs and concrete. *Constr Build Mater*  
1352 2021;270:121456.

1353 [168] Zhang F, Wang C, Liu J, Zou X, Sneed LH, Bao Y, et al. Prediction of FRP-concrete  
1354 interfacial bond strength based on machine learning. *Eng Struct* 2023;274:115156.

1355 [169] Chen J, Liu Y. Fatigue modeling using neural networks: A comprehensive review.

1356 Fatigue Fract Eng Mater Struct 2022;45(4):945-79.

1357 [170] Al-Assaf Y, El Kadi H. Fatigue life prediction of composite materials using polynomial

1358 classifiers and recurrent neural networks. Compos Struct 2007;77(4):561-9.

1359 [171] Lyathakula KR, Yuan F-G. A probabilistic fatigue life prediction for adhesively

1360 bonded joints via ANNs-based hybrid model. Int J Fatigue 2021;151:106352.

1361 [172] Silva GC, Beber VC, Pitz DB. Machine learning and finite element analysis: An

1362 integrated approach for fatigue lifetime prediction of adhesively bonded joints. Fatigue

1363 Fract Eng Mater Struct 2021;44(12):3334-48.

1364 [173] Fernandes PHE, Silva GC, Pitz DB, Schnelle M, Koschek K, Nagel C, et al. Data-

1365 Driven, Physics-Based, or Both: Fatigue Prediction of Structural Adhesive Joints by

1366 Artificial Intelligence. Appl Mech 2023;4(1):334-55.

1367 [174] Yao C, Qi Z, Chen W. Fatigue behavior analysis and life prediction of all-composite

1368 joint. Thin-Walled Struct 2023;183:110320.

1369 [175] Cristiani D, Falchetto F, Yue N, Sbarufatti C, Di Sante R, Zarouchas D, et al. Strain-

1370 based delamination prediction in fatigue loaded CFRP coupon specimens by deep

1371 learning and static loading data. Compos B Eng 2022;241:110020.

1372 [176] Canyurt OE, Meran C. Fatigue strength estimation of adhesively bonded tongue and

1373 groove joint of thick woven composite sandwich structures using genetic algorithm

1374 approach. Int J Adhes Adhes 2012;33:80-8.

1375 [177] Liu H, Liu S, Liu Z, Mrad N, Dong H. Prognostics of damage growth in composite

1376 materials using machine learning techniques. 2017 IEEE International Conference on

1377 Industrial Technology (ICIT): IEEE; 2017. p. 1042-7.

1378 [178] Dabutar S, Ekwaro-Osire S, Dias JP. Fatigue damage diagnostics of composites using  
1379 data fusion and data augmentation with deep neural networks. *J Nondestruct Eval*  
1380 *Diagn Progn Eng Syst* 2022;5(2):021004.

1381 [179] Lee H, Lim HJ, Skinner T, Chattopadhyay A, Hall A. Automated fatigue damage  
1382 detection and classification technique for composite structures using Lamb waves and  
1383 deep autoencoder. *Mech Syst Signal Process* 2022;163:108148.

1384 [180] Azzizadenesheli K, Kovachki N, Li Z, Liu-Schiavini M, Kossaifi J, Anandkumar A.  
1385 Neural Operators for Accelerating Scientific Simulations and Design. *arXiv preprint*  
1386 *arXiv:230915325* 2023.

1387 [181] Wang B, Zhong S, Lee T-L, Fancey KS, Mi J. Non-destructive testing and evaluation  
1388 of composite materials/structures: A state-of-the-art review. *Adv Mech Eng*  
1389 2020;12(4):1687814020913761.

1390 [182] Azad MM, Kim S, Cheon YB, Kim HS. Intelligent structural health monitoring of  
1391 composite structures using machine learning, deep learning, and transfer learning: a  
1392 review. *Adv Compos Mater* 2023:1-27.

1393 [183] Chen J, Yu Z, Jin H. Nondestructive testing and evaluation techniques of defects in  
1394 fiber-reinforced polymer composites: A review. *Front Mater* 2022;9:986645.

1395 [184] Sikdar S, Liu D, Kundu A. Acoustic emission data based deep learning approach for  
1396 classification and detection of damage-sources in a composite panel. *Compos B Eng*  
1397 2022;228:109450.

1398 [185] Dabutar S, Ekwaro-Osire S, Dias JP. Damage classification of composites based on  
1399 analysis of lamb wave signals using machine learning. *ASCE-ASME J Risk Uncertain*  
1400 *Eng Syst B: Mech Eng* 2021;7(1):011002.

1401 [186] Wu J, Xu X, Liu C, Deng C, Shao X. Lamb wave-based damage detection of composite  
1402 structures using deep convolutional neural network and continuous wavelet transform.  
1403 Compos Struct 2021;276:114590.

1404 [187] Mardanshahi A, Nasir V, Kazemirad S, Shokrieh M. Detection and classification of  
1405 matrix cracking in laminated composites using guided wave propagation and artificial  
1406 neural networks. Compos Struct 2020;246:112403.

1407 [188] Hu C, Yang B, Yang L, Wang Z, Hu W, Biao X, et al. Anti-interference damage  
1408 localization in composite overwrapped pressure vessels using machine learning and  
1409 ultrasonic guided waves. NDT & E Int 2023;140:102961.

1410 [189] Fotouhi S, Pashmforoush F, Bodaghi M, Fotouhi M. Autonomous damage recognition  
1411 in visual inspection of laminated composite structures using deep learning. Compos  
1412 Struct 2021;268:113960.

1413 [190] Niccolai A, Caputo D, Chieco L, Grimaccia F, Mussetta M. Machine learning-based  
1414 detection technique for NDT in industrial manufacturing. Mathematics  
1415 2021;9(11):1251.

1416 [191] D'Angelo G, Cavaccini G, Rampone S. Shimming analysis of carbon-fiber composite  
1417 materials with eddy current testing. In: Proceedings of 2018 5th IEEE International  
1418 Workshop on Metrology for AeroSpace (MetroAeroSpace). 2018. p. 68-73.

1419 [192] Marani R, Palumbo D, Galietti U, Stella E, D'Orazio T. Automatic detection of  
1420 subsurface defects in composite materials using thermography and unsupervised  
1421 machine learning. In: Proceedings of 2016 IEEE 8th international conference on  
1422 intelligent systems (IS). 2016. p. 516-21.

1423 [193] Daghig V, Naraghi M. Machine learning-based defect characterization in anisotropic  
1424 materials with IR-thermography synthetic data. Compos Sci Technol 2023;233:109882.

1425 [194] Tong Z, Cheng L, Xie S, Kersemans M. A flexible deep learning framework for  
1426 thermographic inspection of composites. *NDT & E Int* 2023;139:102926.

1427 [195] Fröhlich HB, Fantin AV, de Oliveira BCF, Willemann DP, Iervolino LA, Benedet ME,  
1428 et al. Defect classification in shearography images using convolutional neural  
1429 networks. In: *Proceedings of 2018 International Joint Conference on Neural Networks*  
1430 (IJCNN). 2018. p. 1-7.

1431 [196] Wang Y, Luo Q, Xie H, Li Q, Sun G. Digital image correlation (DIC) based damage  
1432 detection for CFRP laminates by using machine learning based image semantic  
1433 segmentation. *Int J Mech Sci* 2022;230:107529.

1434 [197] Jia Y, Yu G, Du J, Gao X, Song Y, Wang F. Adopting traditional image algorithms and  
1435 deep learning to build the finite model of a 2.5 D composite based on X-Ray computed  
1436 tomography. *Compos Struct* 2021;275:114440.

1437 [198] Gillespie DI, Hamilton AW, Atkinson RC, Bellekens X, Michie C, Andonovic I, et al.  
1438 Composite laminate delamination detection using transient thermal conduction profiles  
1439 and machine learning based data analysis. *Sensors* 2020;20(24):7227.

1440 [199] Brotherhood C, Drinkwater B, Dixon S. The detectability of kissing bonds in adhesive  
1441 joints using ultrasonic techniques. *Ultrasonics* 2003;41(7):521-9.

1442 [200] Yilmaz B, Jasiūnienė E. Advanced ultrasonic NDT for weak bond detection in  
1443 composite-adhesive bonded structures. *Int J Adhes Adhes* 2020;102:102675.

1444 [201] Yilmaz B, Smagulova D, Jasiuniene E. Model-assisted reliability assessment for  
1445 adhesive bonding quality evaluation with ultrasonic NDT. *NDT & E Int*  
1446 2022;126:102596.

1447 [202] Attar L, El Kettani MEC, Leduc D, Predoi MV, Galy J. Detection of kissing bond type  
1448 defects and evaluation of the bonding quality in metal/adhesive/composite structures by  
1449 a wavenumber-frequency insensitive SH mode. *NDT & E Int* 2023;137:102841.

1450 [203] Piao G, Mateus J, Li J, Pachha R, Walia P, Deng Y, et al. Phased array ultrasonic  
1451 imaging and characterization of adhesive bonding between thermoplastic composites  
1452 aided by machine learning. *Nondestruct Test Evaluation* 2023;38(3):500-18.

1453 [204] Li J, Gopalakrishnan K, Piao G, Pacha R, Walia P, Deng Y, et al. Classification of  
1454 adhesive bonding between thermoplastic composites using ultrasonic testing aided by  
1455 machine learning. *Int J Adhes Adhes* 2023:103427.

1456 [205] Qing X, Liao Y, Wang Y, Chen B, Zhang F, Wang Y. Machine learning based  
1457 quantitative damage monitoring of composite structure. *Int J Smart Nano Mater*  
1458 2022;13(2):167-202.

1459 [206] Rytter A. Vibrational based inspection of civil engineering structures [PhD thesis].  
1460 Aalborg, North Jutland Region, Denmark: Aalborg University; 1993.

1461 [207] Ooijevaar TH. Vibration based structural health monitoring of composite skin-stiffener  
1462 structures [PhD thesis]. Enschede, The Netherlands: University of Twente; 2014.

1463 [208] Zhuang Y, Kopsaftopoulos F, Dugnani R, Chang F-K. Integrity monitoring of  
1464 adhesively bonded joints via an electromechanical impedance-based approach. *Struct*  
1465 *Health Monit* 2018;17(5):1031-45.

1466 [209] Bekas DG, Sharif-Khodaei Z, Baltzis D, Aliabadi MF, Paipetis AS. Quality assessment  
1467 and damage detection in nanomodified adhesively-bonded composite joints using  
1468 inkjet-printed interdigital sensors. *Compos Struct* 2019;211:557-63.

1469 [210] Luan C, Yao X, Zhang C, Wang B, Fu J. Large-scale deformation and damage  
1470 detection of 3D printed continuous carbon fiber reinforced polymer-matrix composite  
1471 structures. *Compos Struct* 2019;212:552-60.

1472 [211] Todoroki A, Yamada K, Mizutani Y, Suzuki Y, Matsuzaki R. Impact damage detection  
1473 of a carbon-fibre-reinforced-polymer plate employing self-sensing time-domain  
1474 reflectometry. *Compos Struct* 2015;130:174-9.

1475 [212] Steinbild PJ, Höhne R, Füßel R, Modler N. A sensor detecting kissing bonds in  
1476 adhesively bonded joints using electric time domain reflectometry. *NDT & E Int*  
1477 2019;102:114-9.

1478 [213] Shin C-S, Lin T-C. Adhesive Joint Integrity Monitoring Using the Full Spectral  
1479 Response of Fiber Bragg Grating Sensors. *Polymers* 2021;13(17):2954.

1480 [214] Liu P, Xu D, Li J, Chen Z, Wang S, Leng J, et al. Damage mode identification of  
1481 composite wind turbine blade under accelerated fatigue loads using acoustic emission  
1482 and machine learning. *Struct Health Monit* 2020;19(4):1092-103.

1483 [215] Khan A, Khalid S, Raouf I, Sohn J-W, Kim H-S. Autonomous assessment of  
1484 delamination using scarce raw structural vibration and transfer learning. *Sensors*  
1485 2021;21(18):6239.

1486 [216] Reis PA, Iwasaki KM, Voltz LR, Cardoso EL, Medeiros RD. Damage detection of  
1487 composite beams using vibration response and artificial neural networks. *Proc Inst*  
1488 *Mech Eng Part L J Mater Des Appl* 2022;236(7):1419-30.

1489 [217] Zhou Z-H. A brief introduction to weakly supervised learning. *Natl Sci Rev*  
1490 2018;5(1):44-53.

1491 [218] Marino S, Beauseroy P, Smolarz A. Weakly-supervised learning approach for potato  
1492 defects segmentation. *Eng Appl Artif Intell* 2019;85:337-46.

1493 [219] Liu H, Liu Z, Jia W, Zhang D, Tan J. A novel imbalanced data classification method  
1494 based on weakly supervised learning for fault diagnosis. *IEEE Trans Industr Inform*  
1495 2021;18(3):1583-93.

1496 [220] Alenezi DF, Shi H, Li J. A Ranking-based Weakly Supervised Learning model for  
1497 telemonitoring of Parkinson's disease. *IISE Trans Healthc Syst Eng* 2022;12(4):322-  
1498 36.

1499 [221] Alenezi DF, Biehler M, Shi J, Li J. Physics-Informed Weakly-Supervised Learning for  
1500 Quality Prediction of Manufacturing Processes. *IEEE Trans Autom Sci Eng* 2024.

1501 [222] Nemanic V, Biggio L, Huan X, Hu Z, Fink O, Tran A, et al. Uncertainty quantification  
1502 in machine learning for engineering design and health prognostics: A tutorial. *Mech  
1503 Syst Signal Process* 2023;205:110796.

1504 [223] Li L, Fan Y, Tse M, Lin K-Y. A review of applications in federated learning. *Comput  
1505 Ind Eng* 2020;149:106854.

1506 [224] Li Z, Zheng H, Kovachki N, Jin D, Chen H, Liu B, et al. Physics-informed neural  
1507 operator for learning partial differential equations. *arXiv preprint arXiv:211103794*  
1508 2021.

1509 [225] Wang S, Wang H, Perdikaris P. Learning the solution operator of parametric partial  
1510 differential equations with physics-informed DeepONets. *Sci Adv* 2021;7(40):8605.

1511 [226] Goswami S, Bora A, Yu Y, Karniadakis GE. Physics-informed deep neural operator  
1512 networks. In: *Machine Learning in Modeling and Simulation: Methods and  
1513 Applications*: Springer; 2023. p. 219-54.

1514 [227] Chen RT, Rubanova Y, Bettencourt J, Duvenaud DK. Neural ordinary differential  
1515 equations. *Adv Neural Inf Process Syst* 2018;31.

1516 [228] Finn C, Abbeel P, Levine S. Model-agnostic meta-learning for fast adaptation of deep  
1517 networks. *International Conference on Machine Learning*: PMLR; 2017. p. 1126-35.

1518 [229] Vuorio R, Sun S-H, Hu H, Lim JJ. Multimodal model-agnostic meta-learning via task-  
1519 aware modulation. *Adv Neural Inf Process Syst* 2019;32.

1520 [230] Abdollahzadeh M, Malekzadeh T, Cheung N-MM. Revisit multimodal meta-learning  
1521 through the lens of multi-task learning. *Adv Neural Inf Process Syst* 2021;34:14632-44.

1522 [231] Chen J, Liu Z, Wang K, Jiang C, Zhang C, Wang B. A calibration-free method for  
1523 biosensing in cell manufacturing. *IISE Trans* 2021;54(1):29-39.

1524 [232] LLorca J, González C, Molina-Aldareguía JM, Lopes C. Multiscale modeling of  
1525 composites: toward virtual testing... and beyond. *JOM* 2013;65:215-25.

1526 [233] Rueda-Ruiz M, Herráez M, Sket F, Gálvez F, González C, Molina-Aldareguía JM.  
1527 Study of the effect of strain rate on the in-plane shear and transverse compression  
1528 response of a composite ply using computational micromechanics. *Compos A Appl Sci*  
1529 *Manuf* 2023;168:107482.

1530 [234] Romanowicz M. A mesoscale study of failure mechanisms in angle-ply laminates  
1531 under tensile loading. *Compos B Eng* 2016;90:45-57.

1532 [235] Tavares RP, Melro AR, Bessa MA, Turon A, Liu WK, Camanho PP. Mechanics of  
1533 hybrid polymer composites: analytical and computational study. *Comput Mech*  
1534 2016;57:405-21.

1535 [236] Liu X, Zhou X-Y, Liu B, Gao C. Multiscale modeling of woven composites by deep  
1536 learning neural networks and its application in design optimization. *Compos Struct*  
1537 2023;324:117553.

1538 [237] Bishara D, Xie Y, Liu WK, Li S. A state-of-the-art review on machine learning-based  
1539 multiscale modeling, simulation, homogenization and design of materials. *Arch*  
1540 *Comput Methods Eng* 2023;30(1):191-222.

1541 [238] Ghane E, Fagerström M, Mirkhalaf S. A multiscale deep learning model for elastic  
1542 properties of woven composites. *Int J Solids Struct* 2023;282:112452.

1543 [239] Wei H, Wu C, Hu W, Su T-H, Oura H, Nishi M, et al. LS-DYNA machine learning-  
1544 based multiscale method for nonlinear modeling of short fiber-reinforced composites. *J*  
1545 *Eng Mech* 2023;149(3):04023003.

1546 [240] Lino M, Cantwell C, Bharath AA, Fotiadis S. Simulating continuum mechanics with  
1547 multi-scale graph neural networks. *arXiv preprint arXiv:210604900* 2021.

1548